J Sci Comput
DOI 10.1007/s10915-008-9203-y

Finite Element Approximation of a Three Dimensional Phase Field Model for Void Electromigration

Ľubomír Baňas · Robert Nürnberg

Received: 2 February 2007 / Revised: 10 April 2008 / Accepted: 28 April 2008

Abstract We consider a finite element approximation of a phase field model for the evolution of voids by surface diffusion in an electrically conducting solid. The phase field equations are given by the nonlinear degenerate parabolic system

$$\gamma \frac{\partial u}{\partial t} - \nabla.(b(u)\nabla[w + \alpha\phi]) = 0, \qquad w = -\gamma\,\Delta u + \gamma^{-1}\Psi'(u), \qquad \nabla.(c(u)\nabla\phi) = 0$$

subject to an initial condition $u^0(\cdot) \in [-1, 1]$ on u and flux boundary conditions on all three equations. Here $\gamma \in \mathbb{R}_{>0}$, $\alpha \in \mathbb{R}_{\geq 0}$, Ψ is a non-smooth double well potential, and $c(u) := 1 + u$, $b(u) := 1 - u^2$ are degenerate coefficients. On extending existing results for the simplified two dimensional phase field model, we show stability bounds for our approximation and prove convergence, and hence existence of a solution to this nonlinear degenerate parabolic system in three space dimensions. Furthermore, a new iterative scheme for solving the resulting nonlinear discrete system is introduced and some numerical experiments are presented.

Keywords Void electromigration · Surface diffusion · Phase field model · Degenerate Cahn–Hilliard equation · Fourth order degenerate parabolic system · Finite elements · Convergence analysis · Multigrid methods

1 Introduction

In the recent paper [9], abbreviated to BNS throughout this paper, the authors proposed and analysed a fully practical finite element approximation for a phase field model describing

L. Baňas was supported by the EPSRC grant EP/C548973/1.

L. Baňas · R. Nürnberg (✉)
Department of Mathematics, Imperial College London, London, SW7 2AZ, UK
e-mail: robert.nurnberg@imperial.ac.uk

Present address:
L. Baňas
Department of Mathematics, Heriot-Watt University, Edinburgh, EH14 4AS, UK
e-mail: l.banas@hw.ac.uk

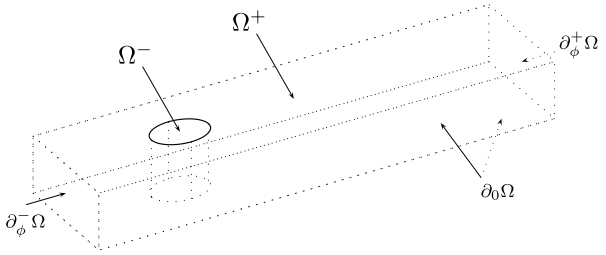

Fig. 1 A sketch of the domain $\Omega \subset \mathbb{R}^3$

void electromigration. The authors restricted their model and their analysis to two spatial dimensions. However, the presented phase field model immediately carries over to three space dimensions, and it is the aim of this paper to extend their finite element approximation and their analysis to this case. Further, we aim at providing a computational method suitable for large scale three dimensional problems.

Let the domain $\Omega := (-L_1, L_1) \times (-L_2, L_2) \times (-L_3, L_3)$ in the shape of a rectangular prism in $\mathbb{R}^d$, $d = 3$, represent the interconnect line, with boundary $\partial\Omega$. At any time $t \in [0, T]$, let the region occupied by the void be $\Omega^-(t) \subset\subset \Omega$ with boundary $\Gamma(t)$. Then the electric field in the conducting region, $\Omega^+(t) := \Omega \setminus \overline{\Omega^-(t)}$, is $E = -\nabla\phi$, where the potential ϕ at any time $t \in [0, T]$ satisfies

$$\Delta\phi = 0 \quad \text{in } \Omega^+(t), \qquad \frac{\partial\phi}{\partial\nu_{\Gamma(t)}} = 0 \quad \text{on } \Gamma(t), \tag{1.1a}$$

$$\frac{\partial\phi}{\partial\nu} = 0 \quad \text{on } \partial_0\Omega, \qquad 2\frac{\partial\phi}{\partial\nu} + \phi = g^\pm := x_1 \pm 2 \quad \text{on } \partial_\phi^\pm\Omega; \tag{1.1b}$$

$\nu_{\Gamma(t)}$ being the unit normal to $\Gamma(t)$ pointing into $\Omega^-(t)$. In the above $\partial\Omega = \partial_0\Omega \cup \partial_\phi\Omega$, where $\partial_0\Omega \cap \partial_\phi\Omega = \emptyset$ and

$$\partial_\phi\Omega = \partial_\phi^-\Omega \cup \partial_\phi^+\Omega \quad \text{with } \partial_\phi^\pm\Omega := \{\pm L_1\} \times [-L_2, L_2] \times [-L_3, L_3],$$

and ν is the outward unit normal to $\partial\Omega$; see the sketch in Fig. 1. Hence $\partial_0\Omega$ is the insulated boundary of Ω, whilst the Robin boundary conditions on the ends $\partial_\phi^\pm\Omega$ model a uniform parallel electric field, $\phi \approx x_1$ as $L_1 \to \infty$. The motion of the void boundary, $\Gamma(t)$, then evolves according to the law

$$V = -\Delta_s[\alpha_1\kappa - \alpha_2\phi] \quad \text{on } \Gamma(t), \tag{1.2}$$

where V is the velocity of $\Gamma(t)$ in the direction of $\nu_{\Gamma(t)}$, Δ_s is the surface Laplacian, and κ is the mean curvature of $\Gamma(t)$ (positive where $\Omega^-(t)$ is convex). Here $\alpha_1 \in \mathbb{R}_{>0}$ and $\alpha_2 \in \mathbb{R}_{\geq 0}$ are given parameters depending on the conductor. The first term on the right hand side of (1.2) is surface diffusion due to interfacial tension, which models atoms moving around the boundary to positions of large curvature; whereas the second term is surface diffusion due to the electric field. The void electromigration model is then the coupled system (1.1a,b) and (1.2). For further details on void electromigration we refer to BNS and the references therein.

To our knowledge, the only numerical results on void electromigration in three space dimensions in the current literature can be found in [34], where a direct approximation of (1.1a,b) and (1.2) is considered. In addition, the authors very recently presented some numerical simulations for the phase field model considered in this paper in [2]. The method

in [34] involves the explicit tracking and meshing of the approximate void boundary, which is given by a two dimensional hypersurface, approximating surface derivatives on it and the remeshing of the approximation to $\Omega^+(t)$ in order to approximate ϕ. This direct approach breaks down at singularities, where there is a change in topology of the interface due to either the break up or the coalescence of voids. In this paper we will consider a phase field model of the original "sharp interface" void electromigration model (1.1a,b) and (1.2). The advantage of a phase field method is that the interface is implicitly embedded and is not tracked explicitly. Moreover, this approach can cope with the voids changing topology. This represents a clear advantage over current computational methods for the sharp interface problem, as these are not able to cope with topological changes of the solution. This limits their use in complex practical situations, where topological changes have to be expected. See Sect. 5 for several examples.

If $\alpha_2 = 0$, then the law of motion (1.2) simplifies to motion by surface diffusion. This geometric evolution equation was originally proposed by Mullins, [28], as an evolution law for a free surface enclosing a solid phase, which changes its shape due to the diffusion of atoms along the surface. In the current literature, there exist two approaches to approximate (1.2) with $\alpha_2 = 0$ in three space dimensions. Direct parametric approximations have been studied in e.g. [3, 11, 26, 27], while level set approaches have been considered in e.g. [15, 33]. To our knowledge, there exist no phase field approximations of surface diffusion in three space dimensions in the literature. For a recent overview on the approximation of geometric evolution equations we refer to [16].

In this paper we consider a phase field model that, as the interfacial region's thickness goes to zero, describes the desired law of motion (1.2). We introduce the interfacial parameter $\gamma \in \mathbb{R}_{>0}$ and the conserved order parameter $u_\gamma(\cdot,t) \in \mathcal{K} := [-1,1] \subset \mathbb{R}$, where at any time $t \in [0,T]$ $u_\gamma(\cdot,t) = -1$ denotes the void and $u_\gamma(\cdot,t) = +1$ denotes the conductor, while the void boundary is approximated by the $u_\gamma(\cdot,t) = 0$ contour surface inside the $|u_\gamma(\cdot,t)| < 1$ interfacial region. We introduce also the chemical potential $w_\gamma(\cdot,t)$ and the electric potential $\phi_\gamma(\cdot,t)$. The sharp interface model, (1.1a,b) and (1.2), is then approximated by the following nonlinear degenerate parabolic system:

(P_γ) Find functions $u_\gamma : \Omega \times [0,T] \to \mathcal{K}$ and $w_\gamma, \phi_\gamma : \Omega \times [0,T] \to \mathbb{R}$ such that

$$\gamma \frac{\partial u_\gamma}{\partial t} - \nabla.(b(u_\gamma)\nabla[w_\gamma + \alpha\phi_\gamma]) = 0 \quad \text{in } \Omega_T := \Omega \times (0,T], \tag{1.3a}$$

$$w_\gamma = -\gamma \Delta u_\gamma + \gamma^{-1}\Psi'(u_\gamma) \quad \text{in } \Omega_T, \text{ where } |u_\gamma| < 1, \tag{1.3b}$$

$$u_\gamma(x,0) = u_\gamma^0(x) \in \mathcal{K} \quad \forall x \in \Omega, \tag{1.3c}$$

$$\frac{\partial u_\gamma}{\partial \nu} = b(u_\gamma)\frac{\partial [w_\gamma + \alpha\phi_\gamma]}{\partial \nu} = 0 \quad \text{on } \partial\Omega \times (0,T], \tag{1.3d}$$

$$\nabla.(c(u_\gamma)\nabla\phi_\gamma) = 0 \quad \text{in } \Omega_T, \tag{1.3e}$$

$$c(u_\gamma)\frac{\partial \phi_\gamma}{\partial \nu} = 0 \quad \text{on } \partial_0\Omega \times (0,T], \qquad c(u_\gamma)\frac{\partial \phi_\gamma}{\partial \nu} + \phi_\gamma = g^\pm \quad \text{on } \partial_\phi^\pm\Omega \times (0,T]. \tag{1.3f}$$

In (1.3a–f), $\gamma > 0$ and $\alpha \geq 0$ are given constants and

$$\Psi(s) := \begin{cases} \frac{1}{2}\left(1 - s^2\right) & \text{if } s \in \mathcal{K}, \\ \infty & \text{if } s \notin \mathcal{K}, \end{cases} \tag{1.4}$$

is an obstacle free energy which restricts $u_\gamma(\cdot,\cdot) \in \mathcal{K}$. In addition, we define the degenerate diffusion coefficients

$$c(s) := 1 + s, \quad b(s) := 1 - s^2 = c(s)c(-s) \quad \forall s \in \mathcal{K}. \tag{1.5}$$

If $\alpha = 0$, then (1.3a–d) collapses to (Q_γ), the degenerate Cahn–Hilliard equation. Existence of a solution to (Q_γ), which is a fourth order degenerate parabolic equation for u_γ, can be found in [17]. Moreover, it is shown in [14] by using the techniques of formal asymptotic expansions that the zero level sets of u_γ, the solution to (Q_γ) for a fixed $\gamma > 0$, converge as $\gamma \to 0$ to an interface, $\Gamma(t)$, evolving according to the geometric motion (1.2) with $\alpha_1 = \frac{\pi^2}{16}$ and $\alpha_2 = 0$. Furthermore, on the zero level sets of u_γ the chemical potential w_γ tends to $-\frac{\pi}{4}\kappa$, where κ is the mean curvature, here defined to be the sum of the two principal curvatures, of the limiting interface $\Gamma(t)$. It is a straightforward matter to extend the technique of formal asymptotic expansions in [14] for (Q_γ) to (P_γ) and one obtains that the zero level sets of u_γ, the solution to (P_γ) for a fixed $\gamma > 0$, converge as $\gamma \to 0$ to an interface, $\Gamma(t)$, evolving according to the modified motion

$$V = -\frac{\pi}{4}\Delta_s\left[\frac{\pi}{4}\kappa - \alpha\phi\right] \quad \text{on } \Gamma(t), \tag{1.6}$$

i.e. (1.2) with $\alpha_1 = \frac{\pi^2}{16}$ and $\alpha_2 = \frac{\pi\alpha}{4}$; see [29] for details. Hence the limiting sharp interface motion of (P_γ) is the void electromigration model, (1.1a,b) and (1.2), for a suitable choice of α and on rescaling time. We remark that for both (P_γ) and (Q_γ) the formal asymptotics yield that the interface thickness is approximately $\gamma\pi$.

We should stress that the numerical analysis of nonlinear degenerate parabolic equations of fourth order, e.g. (P_γ) and (Q_γ), in multiple space dimensions was made feasible only very recently, when Grün, [22], proved convergence in space dimensions $d = 2$ and 3 of a finite element approximation to the thin film equation. E.g. the convergence results for approximations of degenerate Cahn–Hilliard systems in [4, 6, 7] are all restricted to one space dimension. However, in BNS the authors adapted the techniques in [6, 7, 22] to propose and prove convergence of a finite element approximation of (P_γ) for $d = 2$. It is the aim of this paper to extend this analysis to three space dimensions. In doing so, we will prove for a fixed $\gamma > 0$ that the solutions of a finite element approximation of (P_γ) converge, as $h \to 0$, to a weak solution of the problem (P_γ). Of course, given that (P_γ) is a phase field model for the original sharp interface problem (1.1a,b) and (1.2), the ultimate goal would be to show convergence of the discrete solutions to the sharp interface solutions as $\gamma, h \to 0$. To our knowledge, the only result in this direction in the literature can be found in [18], where the authors show such a convergence for the finite element solutions of the nondegenerate Cahn–Hilliard equation, i.e. (Q_γ) with $b(u) = 1$ and a smooth double well potential Ψ, to the corresponding sharp interface limit, the so-called Hele–Shaw problem. For the more complicated degenerate systems (P_γ) and (Q_γ) this remains an open problem.

We now recall some formal energy estimates from BNS that motivate the convergence analysis in Sect. 3. As the analysis in this paper is for a fixed γ, for the remainder of this paper we drop the γ subscripts in (P_γ) for notational convenience. First, we relate F to c and G to b by the identities

$$c(s)F''(s) = 1 \quad \text{and} \quad b(s)G''(s) = 1. \tag{1.7}$$

Then testing (1.3e) with ϕ yields that

$$\int_\Omega c(u)|\nabla\phi|^2\,\mathrm{d}x + \frac{1}{2}\int_{\partial_\phi\Omega}\phi^2\,\mathrm{d}s \le \frac{1}{2}\int_{\partial_\phi\Omega} g^2\,\mathrm{d}s, \tag{1.8}$$

where $g := g^\pm \equiv \pm(2+L_1)$ on $\partial_\phi^\pm\Omega$. Testing (1.3e) with $F'(u)$ and noting (1.7) and (1.8) yields that

$$\left|\int_\Omega \nabla\phi.\nabla u\mathrm{d}x\right| = \left|\int_\Omega c(u)\nabla\phi.\nabla[F'(u)]\mathrm{d}x\right| \le 2\left[\int_{\partial_\phi\Omega} g^2\mathrm{d}s\right]^{\frac{1}{2}}\left[\int_{\partial_\phi\Omega}[F'(u)]^2\mathrm{d}s\right]^{\frac{1}{2}}. \tag{1.9}$$

Testing (1.3a) with w and (1.3b) with $\frac{\partial u}{\partial t}$, combining and noting (1.5) and (1.8) yields that

$$\begin{aligned}
&\frac{\mathrm{d}}{\mathrm{d}t}\int_\Omega\left[\frac{1}{2}\gamma|\nabla u|^2+\gamma^{-1}\Psi(u)\right]\mathrm{d}x + \frac{1}{2}\gamma^{-1}\int_\Omega b(u)|\nabla w|^2\mathrm{d}x\\
&\quad\le \frac{1}{2}\alpha^2\gamma^{-1}\int_\Omega b(u)|\nabla\phi|^2\mathrm{d}x \le \alpha^2\gamma^{-1}\int_\Omega c(u)|\nabla\phi|^2\mathrm{d}x\\
&\quad\le \frac{1}{2}\alpha^2\gamma^{-1}\int_{\partial_\phi\Omega} g^2\mathrm{d}s.
\end{aligned} \tag{1.10}$$

Testing (1.3a) with $G'(u)$ and (1.3b) with $-\Delta u$, combining and noting (1.7), (1.4) and (1.9) yields that

$$\begin{aligned}
&\gamma\frac{\mathrm{d}}{\mathrm{d}t}\int_\Omega G(u)\mathrm{d}x + \gamma\int_\Omega|\Delta u|^2\mathrm{d}x\\
&\quad\le \int_\Omega \nabla(\gamma^{-1}u-\alpha\phi).\nabla u\mathrm{d}x\\
&\quad\le \gamma^{-1}\int_\Omega|\nabla u|^2\mathrm{d}x + 2\alpha\left[\int_{\partial_\phi\Omega} g^2\mathrm{d}s\right]^{\frac{1}{2}}\left[\int_{\partial_\phi\Omega}[F'(u)]^2\mathrm{d}s\right]^{\frac{1}{2}}.
\end{aligned} \tag{1.11}$$

From (1.11) and (1.10) one can formally show that $u \in L^2(0,T;H^2(\Omega))$ if $u(\cdot,0)\in\mathcal{K}$, and hence $u(\cdot,t)\in C^{0,\frac{1}{2}}(\overline{\Omega})$ for almost all $t\in(0,T)$. We stress that these estimates are merely formal, and in particular a regularization procedure is needed to make the derivation rigorous. But they serve as a motivation for the procedure in the discrete case, where the analogue to (1.11), see (2.27) below, will play a crucial role in establishing that the limiting solutions are continuous, see e.g. (3.10d) below. To this end, and following BNS, we will introduce a finite element approximation of (P) that is consistent with the energy estimates (1.8)–(1.11).

This paper is organised as follows. In Sect. 2 we formulate a fully practical finite element approximation of the degenerate system (P) and derive discrete analogues of the energy estimates (1.8)–(1.11). In Sect. 3 we prove convergence, and hence existence of a solution to the system (P) in three space dimensions. In Sect. 4 we describe a new iterative scheme for solving the nonlinear discrete system for the approximations of u and w at each time level. The method is based on the "Uzawa type" iterative solver in [21], and as it uses multigrid solvers for the relevant subproblems, it is superior to the standard block "Gauss–Seidel type" iterative scheme considered in BNS. Finally, in Sect. 5 we present numerous numerical experiments.

Notation and Auxiliary Results

For $D \subset \mathbb{R}^d$, $d = 2, 3$, we adopt the standard notation for Sobolev spaces, denoting the norm of $W^{m,q}(D)$ ($m \in \mathbb{N}$, $q \in [1, \infty]$) by $\|\cdot\|_{m,q,D}$ and the semi-norm by $|\cdot|_{m,q,D}$. We extend these norms and semi-norms in the natural way to the corresponding spaces of vector and matrix valued functions. For $q = 2$, $W^{m,2}(D)$ will be denoted by $H^m(D)$ with the associated norm and semi-norm written as, respectively, $\|\cdot\|_{m,D}$ and $|\cdot|_{m,D}$. For notational convenience, we drop the domain subscript on the above norms and semi-norms in the case $D \equiv \Omega$. Throughout $(\cdot, \cdot)$ denotes the standard L^2 inner product over Ω. In addition we define $\fint \eta := \frac{1}{m(\Omega)}(\eta, 1)$ for all $\eta \in L^1(\Omega)$.

For later purposes, we recall the following compactness results. Let X, Y and Z be Banach spaces with a compact embedding $X \hookrightarrow Y$ and a continuous embedding $Y \hookrightarrow Z$. Then the embeddings

$$\left\{\eta \in L^2(0,T;X) : \frac{\partial \eta}{\partial t} \in L^2(0,T;Z)\right\} \hookrightarrow L^2(0,T;Y) \tag{1.12a}$$

and

$$\left\{\eta \in L^\infty(0,T;X) : \frac{\partial \eta}{\partial t} \in L^2(0,T;Z)\right\} \hookrightarrow C([0,T];Y) \tag{1.12b}$$

are compact, see [32].

It is convenient to introduce the "inverse Laplacian" operator $\mathcal{G} : Y \to Z$ such that

$$(\nabla[\mathcal{G}z], \nabla\eta) = \langle z, \eta\rangle \quad \forall \eta \in H^1(\Omega), \tag{1.13}$$

where $Y := \{z \in (H^1(\Omega))' : \langle z, 1\rangle = 0\}$ and $Z := \{z \in H^1(\Omega) : (z, 1) = 0\}$. Here and throughout $\langle\cdot,\cdot\rangle$ denotes the duality pairing between $(H^1(\Omega))'$ and $H^1(\Omega)$.

Throughout C denotes a generic constant independent of h, τ and ε; the mesh and temporal discretization parameters and the regularization parameter. In addition $C(a_1, \ldots, a_I)$ denotes a constant depending on the arguments $\{a_i\}_{i=1}^I$. Furthermore $\cdot^{(\star)}$ denotes an expression with or without the superscript $\star$. Finally, we define for any $s \in \mathbb{R}$

$$[s]_- := \min\{s, 0\}, \qquad [s]_+ := \max\{s, 0\}, \qquad [s]_{\mathcal{K}} := \max\{-1, \min\{s, 1\}\}. \tag{1.14}$$

2 Finite Element Approximation

We consider the finite element approximation of (P) under the following assumptions on the mesh:

(A) Let Ω be a rectangular prism shaped domain. Let $\{\mathcal{T}^h\}_{h>0}$ be a quasi-uniform family of partitionings of Ω into disjoint open simplices σ with $h_\sigma := \operatorname{diam}(\sigma)$ and $h := \max_{\sigma\in\mathcal{T}^h} h_\sigma$, so that $\overline{\Omega} = \bigcup_{\sigma\in\mathcal{T}^h} \overline{\sigma}$. In addition, it is assumed that all simplices $\sigma \in \mathcal{T}^h$ are generic right-angled simplices, i.e. that all tetrahedra have two vertices at which two edges intersect at right angles.

We note that a cube is easily partitioned into such tetrahedra, see e.g. [13, Fig. 2]. We note furthermore that the right angle constraint on the partitioning is required for our approximations of $b(\cdot)$ and $c(\cdot)$, see (2.8a,b) and (2.5a,b) below.

Associated with $\mathcal{T}^h$ is the finite element space

$$S^h := \{\chi \in C(\overline{\Omega}) : \chi \mid_\sigma \text{ is linear } \forall \sigma \in \mathcal{T}^h\} \subset H^1(\Omega).$$

We introduce also

$$K^h := \{\chi \in S^h : |\chi| \leq 1 \text{ in } \Omega\} \subset K := \{\eta \in H^1(\Omega) : |\eta| \leq 1 \text{ a.e. in } \Omega\}.$$

Let J be the set of nodes of $\mathcal{T}^h$ and $\{p_j\}_{j\in J}$ the coordinates of these nodes. Let $\{\chi_j\}_{j\in J}$ be the standard basis functions for S^h; that is $\chi_j \in S^h$ and $\chi_j(p_i) = \delta_{ij}$ for all $i, j \in J$. We introduce $\pi^h : C(\overline{\Omega}) \to S^h$, the interpolation operator, such that $(\pi^h\eta)(p_j) = \eta(p_j)$ for all $j \in J$. A discrete semi-inner product on $C(\overline{\Omega})$ is then defined by

$$(\eta_1, \eta_2)^h := \int_\Omega \pi^h(\eta_1(x)\eta_2(x))\mathrm{d}x = \sum_{j\in J} m_j \eta_1(p_j)\eta_2(p_j), \tag{2.1}$$

where $m_j := (1, \chi_j) > 0$. The induced discrete semi-norm is then $|\eta|_h := [(\eta, \eta)^h]^{\frac{1}{2}}$, where $\eta \in C(\overline{\Omega})$.

On recalling (1.5) and (1.7), we then define functions F and G such that $c(u)\nabla[F'(u)] = \nabla u$ and $b(u)\nabla[G'(u)] = \nabla u$; that is,

$$F''(s) = \frac{1}{c(s)} = \frac{1}{1+s} \quad \text{and} \quad G''(s) = \frac{1}{b(s)} = \frac{1}{c(s)c(-s)} = \frac{1}{1-s^2}. \tag{2.2}$$

We take $F, G \in C^\infty(-1, 1)$, such that

$$F(s) = (1+s)\log\left(\frac{1+s}{2}\right) + (1-s) \quad \text{and} \quad G(s) = \frac{1}{2}[F(s) + F(-s)]; \tag{2.3}$$

and, for computational purposes, we replace F, G for any $\varepsilon \in (0, 1)$ by the regularized functions $F_\varepsilon, G_\varepsilon : \mathbb{R} \to \mathbb{R}$ such that

$$\begin{aligned} F_\varepsilon(s) &:= \begin{cases} F(\varepsilon-1) + (s-\varepsilon+1)F'(\varepsilon-1) + \frac{(s-\varepsilon+1)^2}{2}F''(\varepsilon-1) & s \leq \varepsilon - 1 \\ F(s) & s \geq \varepsilon - 1 \end{cases}, \\ G_\varepsilon(s) &:= \frac{1}{2}[F_\varepsilon(s) + F_\varepsilon(-s)]. \end{aligned} \tag{2.4}$$

Similarly to the approach in BNS, we introduce $\Lambda_\varepsilon : S^h \to [L^\infty(\Omega)]^{3\times 3}$ such that for all $z^h \in S^h$ and a.e. in Ω

$$\Lambda_\varepsilon(z^h) \text{ is symmetric and positive semi-definite,} \tag{2.5a}$$

$$\Lambda_\varepsilon(z^h)\nabla\pi^h[F'_\varepsilon(z^h)] = \nabla z^h. \tag{2.5b}$$

We now give the construction of Λ_ε, which is the natural extension of the construction given in BNS for $d = 2$. Let $\{e_i\}_{i=1}^3$ be the orthonormal vectors in $\mathbb{R}^3$, such that the jth component of e_i is δ_{ij}, $i, j = 1 \to 3$. Given non-zero constants β_i, $i = 1 \to 3$; let $\hat{\sigma}(\{\beta_i\}_{i=1}^3)$ be the reference open simplex in $\mathbb{R}^3$ with vertices $\{\hat{p}_i\}_{i=0}^3$, where $\hat{p}_0$ is the origin and $\hat{p}_i = \hat{p}_{i-1} + \beta_i e_i$, $i = 1 \to 3$. Given a $\sigma \in \mathcal{T}^h$ with vertices $\{p_{j_i}\}_{i=0}^3$, such that p_{j_0} is not a right-angled vertex, then there exists a rotation matrix R_σ and non-zero constants $\{\beta_i\}_{i=1}^3$ such

that the mapping $\mathcal{R}_\sigma : \hat{x} \in \mathbb{R}^3 \to p_{j_0} + R_\sigma \hat{x} \in \mathbb{R}^3$ maps the vertex $\hat{p}_i$ to p_{j_i}, $i = 0 \to 3$, and hence $\hat{\sigma} \equiv \hat{\sigma}(\{\beta_i\}_{i=1}^3)$ to σ. For any $z^h \in S^h$, we then set

$$\Lambda_\varepsilon(z^h)\mid_\sigma := R_\sigma \hat{\Lambda}_\varepsilon(\hat{z}^h)\mid_{\hat{\sigma}} R_\sigma^T, \tag{2.6}$$

where $\hat{z}^h(\hat{x}) \equiv z^h(\mathcal{R}_\sigma \hat{x})$ for all $\hat{x} \in \overline{\hat{\sigma}}$ and $\hat{\Lambda}_\varepsilon(\hat{z}^h)\mid_{\hat{\sigma}}$ is the 3×3 diagonal matrix with diagonal entries, $k = 1 \to 3$,

$$[\hat{\Lambda}_\varepsilon(\hat{z}^h)\mid_{\hat{\sigma}}]_{kk} := \begin{cases} \frac{\hat{z}^h(\hat{p}_k) - \hat{z}^h(\hat{p}_{k-1})}{F'_\varepsilon(\hat{z}^h(\hat{p}_k)) - F'_\varepsilon(\hat{z}^h(\hat{p}_{k-1}))} \equiv \frac{z^h(p_{j_k}) - z^h(p_{j_{k-1}})}{F'_\varepsilon(z^h(p_{j_k})) - F'_\varepsilon(z^h(p_{j_{k-1}}))} & \text{if } z^h(p_{j_k}) \neq z^h(p_{j_{k-1}}), \\ \frac{1}{F''_\varepsilon(\hat{z}^h(\hat{p}_k))} \equiv \frac{1}{F''_\varepsilon(z^h(p_{j_k}))} & \text{if } z^h(p_{j_k}) = z^h(p_{j_{k-1}}). \end{cases} \tag{2.7}$$

As $R_\sigma^T \equiv R_\sigma^{-1}$, $\nabla z^h \equiv R_\sigma \hat{\nabla} \hat{z}^h$, where $x \equiv (x_1, x_2, x_3)^T$, $\nabla \equiv (\frac{\partial}{\partial x_1}, \frac{\partial}{\partial x_2}, \frac{\partial}{\partial x_3})^T$, $\hat{x} \equiv (\hat{x}_1, \hat{x}_2, \hat{x}_3)^T$ and $\hat{\nabla} \equiv (\frac{\partial}{\partial \hat{x}_1}, \frac{\partial}{\partial \hat{x}_2}, \frac{\partial}{\partial \hat{x}_3})^T$, it easily follows that $\Lambda_\varepsilon(z^h)$ constructed in (2.6) and (2.7) satisfies (2.5a,b). It is this construction that requires the right angle constraint on the partitioning $\mathcal{T}^h$. In a similar fashion we introduce $\Xi_\varepsilon : S^h \to [L^\infty(\Omega)]^{3\times 3}$ such that for all $z^h \in S^h$ and a.e. in Ω

$$\Xi_\varepsilon(z^h) \text{ is symmetric and positive semi-definite,} \tag{2.8a}$$

$$\Xi_\varepsilon(z^h)\nabla \pi^h[G'_\varepsilon(z^h)] = \nabla z^h. \tag{2.8b}$$

We can directly extend the construction (2.6)–(2.7) for Λ_ε to Ξ_ε.

In addition to $\mathcal{T}^h$, let $0 = t_0 < t_1 < \cdots < t_{N-1} < t_N = T$ be a partitioning of $[0, T]$ into possibly variable time steps $\tau_n := t_n - t_{n-1}$, $n = 1 \to N$. We set $\tau := \max_{n=1\to N} \tau_n$. For any given $\varepsilon \in (0, 1)$, we then consider the following fully practical finite element approximation of (P):

$(P_\varepsilon^{h,\tau})$ For $n \geq 1$ find $\{\Phi_\varepsilon^n, U_\varepsilon^n, W_\varepsilon^n\} \in S^h \times K^h \times S^h$ such that

$$(\Lambda_\varepsilon(U_\varepsilon^{n-1})\nabla \Phi_\varepsilon^n, \nabla \chi) + \int_{\partial_\phi \Omega} (\Phi_\varepsilon^n - g)\chi \,\mathrm{d}s = 0 \quad \forall \chi \in S^h, \tag{2.9a}$$

$$\gamma \left(\frac{U_\varepsilon^n - U_\varepsilon^{n-1}}{\tau_n}, \chi \right)^h + (\Xi_\varepsilon(U_\varepsilon^{n-1})\nabla[W_\varepsilon^n + \alpha \Phi_\varepsilon^n], \nabla \chi) = 0 \quad \forall \chi \in S^h, \tag{2.9b}$$

$$\gamma(\nabla U_\varepsilon^n, \nabla[\chi - U_\varepsilon^n]) \geq (W_\varepsilon^n + \gamma^{-1} U_\varepsilon^{n-1}, \chi - U_\varepsilon^n)^h \quad \forall \chi \in K^h, \tag{2.9c}$$

where g as in (1.8) and $U_\varepsilon^0 \in K^h$ is an approximation of $u^0 \in K$, e.g. $U_\varepsilon^0 \equiv \pi^h u^0$ if $u^0 \in C(\overline{\Omega})$.

Below we recall some well-known results concerning S^h for any $\sigma \in \mathcal{T}^h$, $\chi, z^h \in S^h$, $m \in \{0, 1\}$, $p \in [1, \infty]$ and $q \in (3, \infty]$:

$$|\chi|_{1,\sigma} \leq C h_\sigma^{-1} |\chi|_{0,\sigma}; \tag{2.10}$$

$$|\chi|_{m,r,\sigma} \leq C h_\sigma^{-3(\frac{1}{p} - \frac{1}{r})} |\chi|_{m,p,\sigma} \quad \text{for any } r \in [p, \infty]; \tag{2.11}$$

$$|(I - \pi^h)\eta|_m \leq C h^{2-m} |\eta|_2 \quad \forall \eta \in H^2(\Omega); \tag{2.12}$$

$$|(I - \pi^h)\eta|_{m,q} \leq C h^{1-m} |\eta|_{1,q} \quad \forall \eta \in W^{1,q}(\Omega); \tag{2.13}$$

$$\int_\sigma \chi^2 \mathrm{d}x \le \int_\sigma \pi^h[\chi^2]\mathrm{d}x \le 5\int_\sigma \chi^2 \mathrm{d}x; \tag{2.14}$$

$$|(\chi, z^h) - (\chi, z^h)^h| \le |(I-\pi^h)(\chi z^h)|_{0,1} \le Ch^{1+m}|\chi|_m |z^h|_1. \tag{2.15}$$

We introduce the "discrete Laplacian" operator $\Delta^h : S^h \to Z^h := \{z^h \in S^h : (z^h, 1) = 0\}$ such that

$$(\Delta^h z^h, \chi)^h = -(\nabla z^h, \nabla \chi) \quad \forall \chi \in S^h. \tag{2.16}$$

We note for future reference, as we have a quasi-uniform family of partitionings and as Ω is convex, that for all $z^h \in S^h$

$$|z^h|_{1,s} \le C|\Delta^h z^h|_0, \quad \text{for any } s \in (1, 6]; \tag{2.17}$$

see for example [8, Lemma 3.1].

Following BNS, we introduce for all $\varepsilon \in (0,1)$ the regularized functions $c_\varepsilon : \mathcal{K} \to [\varepsilon, 2]$ and $b_\varepsilon : \mathcal{K} \to [\varepsilon(2-\varepsilon), 1]$ defined, on recalling (2.2), (2.4) and (1.14), by

$$c_\varepsilon(s) := [c(s) - \varepsilon]_+ + \varepsilon = \frac{1}{F''_\varepsilon(s)} \ge \frac{1}{F''(s)} = c(s), \tag{2.18a}$$

$$b_\varepsilon(s) := 2\frac{c_\varepsilon(s)c_\varepsilon(-s)}{c_\varepsilon(s) + c_\varepsilon(-s)} = \frac{1}{G''_\varepsilon(s)} \ge \frac{1}{G''(s)} = b(s). \tag{2.18b}$$

Then the following three lemmas hold, see BNS for their proofs, which immediately carry over to three space dimensions and the construction (2.6), (2.7).

Lemma 2.1 *Let the assumptions* (A) *hold. Then for any given* $\varepsilon \in (0,1)$ *the functions* $\Lambda_\varepsilon, \Xi_\varepsilon : S^h \to [L^\infty(\Omega)]^{3\times 3}$ *satisfy for all* $z^h \in K^h$, $\xi \in \mathbb{R}^3$ *and for all* $\sigma \in \mathcal{T}^h$

$$\varepsilon\xi^T\xi \le \min_{x\in\overline{\sigma}} c_\varepsilon(z^h(x))\xi^T\xi \le \xi^T \Lambda_\varepsilon(z^h)\,|_\sigma\, \xi \le \max_{x\in\overline{\sigma}} c_\varepsilon(z^h(x))\xi^T\xi \le 2\xi^T\xi, \tag{2.19a}$$

$$\varepsilon(2-\varepsilon)\xi^T\xi \le \min_{x\in\overline{\sigma}} b_\varepsilon(z^h(x))\xi^T\xi \le \xi^T \Xi_\varepsilon(z^h)\,|_\sigma\, \xi \le \max_{x\in\overline{\sigma}} b_\varepsilon(z^h(x))\xi^T\xi \le \xi^T\xi, \tag{2.19b}$$

$$\xi^T \Xi_\varepsilon(z^h)\,|_\sigma\, \xi \le 2\xi^T \Lambda_\varepsilon(z^h)\,|_\sigma\, \xi. \tag{2.19c}$$

Lemma 2.2 *Let the assumptions* (A) *hold and let* $\|\cdot\|$ *denote the spectral norm on* $\mathbb{R}^{3\times 3}$. *Then for any given* $\varepsilon \in (0,1)$ *the functions* $\Lambda_\varepsilon : S^h \to [L^\infty(\Omega)]^{3\times 3}$ *and* $\Xi_\varepsilon : S^h \to [L^\infty(\Omega)]^{3\times 3}$ *are such that for all* $z^h \in K^h$ *and for all* $\sigma \in \mathcal{T}^h$

$$\max_{x\in\sigma} \|\{\Lambda_\varepsilon(z^h) - c_\varepsilon(z^h)\mathcal{I}\}(x)\| \le h_\sigma |\nabla[c_\varepsilon(z^h)]|_{0,\infty,\sigma} \le h_\sigma |\nabla z^h\,|_\sigma\,|, \tag{2.20a}$$

$$\max_{x\in\sigma} \|\{\Xi_\varepsilon(z^h) - b_\varepsilon(z^h)\mathcal{I}\}(x)\| \le h_\sigma |\nabla[b_\varepsilon(z^h)]|_{0,\infty,\sigma} \le 2h_\sigma |\nabla z^h\,|_\sigma\,|, \tag{2.20b}$$

where $\mathcal{I}$ *is the* 3×3 *identity matrix.*

Lemma 2.3 *Let the assumptions* (A) *hold and* $U_\varepsilon^{n-1} \in K^h$. *Then for all* $\varepsilon \in (0,1)$ *and for all* $h, \tau_n > 0$ *there exists a solution* $\{\Phi_\varepsilon^n, U_\varepsilon^n, W_\varepsilon^n\}$ *to the n-th step of* $(\mathrm{P}_\varepsilon^{h,\tau})$ *with* $\int U_\varepsilon^n = \int U_\varepsilon^{n-1}$. $\{\Phi_\varepsilon^n, U_\varepsilon^n\}$ *is unique. In addition,* W_ε^n *is unique if there exists* $j \in J$ *such that* $U_\varepsilon^n(p_j) \in (-1,1)$. *Moreover, it holds that*

$$(\Lambda_\varepsilon(U_\varepsilon^{n-1})\nabla\Phi_\varepsilon^n, \nabla\Phi_\varepsilon^n) + \frac{1}{2}|\Phi_\varepsilon^n|^2_{0,\partial_\phi\Omega} \le \frac{1}{2}|g|^2_{0,\partial_\phi\Omega}, \tag{2.21}$$

$$|(\nabla\Phi_\varepsilon^n, \nabla U_\varepsilon^{n-1})| \le 2|g|_{0,\partial_\phi\Omega}|\pi^h[F_\varepsilon'(U_\varepsilon^{n-1})]|_{0,\partial_\phi\Omega} \tag{2.22}$$

and

$$\mathcal{E}(U_\varepsilon^n) + \frac{1}{2}\left[\gamma|U_\varepsilon^n - U_\varepsilon^{n-1}|_1^2 + \gamma^{-1}|U_\varepsilon^n - U_\varepsilon^{n-1}|_h^2\right] + \frac{1}{2}\gamma^{-1}\tau_n|[\Xi_\varepsilon(U_\varepsilon^{n-1})]^{\frac{1}{2}}\nabla W_\varepsilon^n|_0^2 \le \mathcal{E}(U_\varepsilon^{n-1}) + \frac{1}{2}\alpha^2\gamma^{-1}\tau_n|g|_{0,\partial_\phi\Omega}^2, \tag{2.23a}$$

where

$$\mathcal{E}(U_\varepsilon^n) := \frac{1}{2}[\gamma|U_\varepsilon^n|_1^2 - \gamma^{-1}|U_\varepsilon^n|_h^2]. \tag{2.23b}$$

Furthermore, it holds that

$$\gamma(G_\varepsilon(U_\varepsilon^n) - G_\varepsilon(U_\varepsilon^{n-1}), 1)^h + \gamma\tau_n|\Delta^h U_\varepsilon^n|_h^2 \le \varepsilon^{-1}\gamma|U_\varepsilon^n - U_\varepsilon^{n-1}|_h^2 + \tau_n(\nabla W_\varepsilon^n, \nabla[U_\varepsilon^n - U_\varepsilon^{n-1}]) + \tau_n(\nabla[\gamma^{-1}U_\varepsilon^n - \alpha\Phi_\varepsilon^n], \nabla U_\varepsilon^{n-1}). \tag{2.24}$$

Remark 2.1 We note that (2.21)–(2.24) are the discrete analogues of the energy estimates (1.8)–(1.11), respectively.

We can now establish that the approximation (2.9a–c) is unconditionally stable.

Theorem 2.1 *Let the assumptions* (A) *hold and* $U_\varepsilon^0 \in K^h$. *Then for all* $\varepsilon \in (0,1)$, $h > 0$ *and for all time partitions* $\{\tau_n\}_{n=1}^N$, *the solution* $\{\Phi_\varepsilon^n, U_\varepsilon^n, W_\varepsilon^n\}_{n=1}^N$ *to* $(\mathrm{P}_\varepsilon^{h,\tau})$ *is such that* $\mathcal{f}U_\varepsilon^n = \mathcal{f}U_\varepsilon^0$, $n = 1 \to N$, *and*

$$\gamma \max_{n=1\to N}\|U_\varepsilon^n\|_1^2 + \sum_{n=1}^N\left[\gamma|U_\varepsilon^n - U_\varepsilon^{n-1}|_1^2 + \gamma^{-1}|U_\varepsilon^n - U_\varepsilon^{n-1}|_0^2\right] + \gamma^{-1}\sum_{n=1}^N\tau_n|[\Xi_\varepsilon(U_\varepsilon^{n-1})]^{\frac{1}{2}}\nabla W_\varepsilon^n|_0^2 \le C\left[\gamma\|U_\varepsilon^0\|_1^2 + \gamma^{-1}(1 + T|g|_{0,\partial_\phi\Omega}^2)\right]. \tag{2.25}$$

In addition

$$\gamma\sum_{n=1}^N\tau_n\left|\mathcal{G}\left[\frac{U_\varepsilon^n - U_\varepsilon^{n-1}}{\tau_n}\right]\right|_1^2 + \gamma\tau^{-\frac{1}{2}}\sum_{n=1}^N|U_\varepsilon^n - U_\varepsilon^{n-1}|_0^2 \le C\left[\gamma\|U_\varepsilon^0\|_1^2 + \gamma^{-1}(1 + T|g|_{0,\partial_\phi\Omega}^2)\right] \tag{2.26}$$

and

$$\gamma \max_{n=1\to N}(G_\varepsilon(U_\varepsilon^n), 1)^h + \gamma\sum_{n=1}^N\tau_n|\Delta^h U_\varepsilon^n|_h^2 \le \gamma(G_\varepsilon(U_\varepsilon^0), 1)^h + \alpha^2\sum_{n=1}^N\tau_n|\pi^h[F_\varepsilon'(U_\varepsilon^{n-1})]|_{0,\partial_\phi\Omega}^2 + C(T)[1 + \gamma^{-2} + \varepsilon^{-1}\tau^{\frac{1}{2}}]\left[\gamma\|U_\varepsilon^0\|_1^2 + \gamma^{-1}(1 + T|g|_{0,\partial_\phi\Omega}^2)\right]. \tag{2.27}$$

Proof The proof is the same as for Theorem 2.6 in BNS. We repeat it here for the reader's convenience. Summing (2.23a) from $n = 1 \to k$ yields for any $k \le N$ that

$$\mathcal{E}(U_\varepsilon^k) + \frac{1}{2}\sum_{n=1}^{k}\left[\gamma|U_\varepsilon^n - U_\varepsilon^{n-1}|_1^2 + \gamma^{-1}|U_\varepsilon^n - U_\varepsilon^{n-1}|_h^2\right]$$
$$+ \frac{1}{2}\gamma^{-1}\sum_{n=1}^{k}\tau_n|[\Xi_\varepsilon(U_\varepsilon^{n-1})]^{\frac{1}{2}}\nabla W_\varepsilon^n|_0^2 \le \mathcal{E}(U_\varepsilon^0) + \frac{1}{2}\alpha^2\gamma^{-1}t_k|g|_{0,\partial_\phi\Omega}^2. \tag{2.28}$$

The desired result (2.25) then follows from (2.28), (2.23b), (2.1), (2.14) and the fact that $U_\varepsilon^n \in K^h$, $n = 0 \to N$.

In order to show (2.26), we introduce the L^2 projection $Q^h : L^2(\Omega) \to S^h$ defined by

$$(Q^h\eta, \chi)^h = (\eta, \chi) \quad \forall \chi \in S^h.$$

Then, from (1.13), (2.9b), (2.19b,c) and assumption (A) we obtain for any $\eta \in H^1(\Omega)$ that

$$\gamma\left(\nabla\mathcal{G}\left[\frac{U_\varepsilon^n - U_\varepsilon^{n-1}}{\tau_n}\right], \nabla\eta\right) = \gamma\left(\frac{U_\varepsilon^n - U_\varepsilon^{n-1}}{\tau_n}, \eta\right) = \gamma\left(\frac{U_\varepsilon^n - U_\varepsilon^{n-1}}{\tau_n}, Q^h\eta\right)^h$$
$$= -(\Xi_\varepsilon(U_\varepsilon^{n-1})\nabla[W_\varepsilon^n + \alpha\Phi_\varepsilon^n], \nabla[Q^h\eta])$$
$$\le \left[|[\Xi_\varepsilon(U_\varepsilon^{n-1})]^{\frac{1}{2}}\nabla W_\varepsilon^n|_0 + \alpha|[\Xi_\varepsilon(U_\varepsilon^{n-1})]^{\frac{1}{2}}\nabla\Phi_\varepsilon^n|_0\right]|Q^h\eta|_1$$
$$\le C\left[|[\Xi_\varepsilon(U_\varepsilon^{n-1})]^{\frac{1}{2}}\nabla W_\varepsilon^n|_0 + \alpha|[\Lambda_\varepsilon(U_\varepsilon^{n-1})]^{\frac{1}{2}}\nabla\Phi_\varepsilon^n|_0\right]|\eta|_1. \tag{2.29}$$

The first bound in (2.26) then follows from (2.29), (2.21) and (2.25). Moreover, we have from (1.13) that

$$\sum_{n=1}^{N}|U_\varepsilon^n - U_\varepsilon^{n-1}|_0^2 \le \tau^{\frac{1}{2}}\left[\sum_{n=1}^{N}|U_\varepsilon^n - U_\varepsilon^{n-1}|_1^2\right]^{\frac{1}{2}}\left[\sum_{n=1}^{N}\tau_n\left|\mathcal{G}[U_\varepsilon^{n-1}\tau_n]\right|_1^2\right]^{\frac{1}{2}}.$$

The second bound in (2.26) then follows from the first and (2.25).

Finally, summing (2.24) from $n = 1 \to k$ and noting (2.1), (2.14) and (2.19b) yields for any $k \le N$ that

$$\gamma(G_\varepsilon(U_\varepsilon^k), 1)^h + \gamma\sum_{n=1}^{k}\tau_n|\Delta^h U_\varepsilon^n|_h^2 \le \gamma(G_\varepsilon(U_\varepsilon^0), 1)^h$$
$$+ \sum_{n=1}^{k}\left[4\varepsilon^{-1}\gamma|U_\varepsilon^n - U_\varepsilon^{n-1}|_0^2 + \alpha\tau_n|(\nabla\Phi_\varepsilon^n, \nabla U_\varepsilon^{n-1})|\right] + \gamma^{-1}t_k\max_{n=0\to k}\|U_\varepsilon^n\|_1^2$$
$$+ \left[\varepsilon^{-1}\sum_{n=1}^{k}\tau_n|[\Xi_\varepsilon(U_\varepsilon^{n-1})]^{\frac{1}{2}}\nabla W_\varepsilon^n|_0^2\right]^{\frac{1}{2}}\left[\sum_{n=1}^{k}\tau_n|U_\varepsilon^n - U_\varepsilon^{n-1}|_1^2\right]^{\frac{1}{2}}. \tag{2.30}$$

The desired result (2.27) then follows from (2.30), (2.22), (2.25) and (2.26). □

Lemma 2.4 *Let $u^0 \in K \cap W^{1,p}(\Omega)$, with $p > 3$, and let the assumptions* (A) *hold. On choosing $U_\varepsilon^0 \equiv \pi^h u^0$ it follows that $U_\varepsilon^0 \in K^h$ is such that for all $h > 0$*

$$\|U_\varepsilon^0\|_1^2 + (G_\varepsilon(U_\varepsilon^0), 1)^h \leq C. \tag{2.31}$$

Proof The desired result (2.31) follows immediately from (2.13), (2.4) and (2.3). □

Remark 2.2 In Sect. 5, we will also consider computations for the following approximation to (P).

($\widetilde{\mathrm{P}}^{h,\tau}$) For $n \geq 1$ find $\{\Phi_\varepsilon^n, U_\varepsilon^n, W_\varepsilon^n\} \in S^h \times K^h \times S^h$ such that

$$(c(U_\varepsilon^{n-1})\nabla\Phi_\varepsilon^n, \nabla\chi) + \int_{\partial_\phi\Omega} (\Phi_\varepsilon^n - g)\chi \,\mathrm{d}s = 0 \quad \forall \chi \in S^h, \tag{2.32a}$$

$$\gamma\left(\frac{U_\varepsilon^n - U_\varepsilon^{n-1}}{\tau_n}, \chi\right)^h + (\pi^h[b(U_\varepsilon^{n-1})]\nabla[W_\varepsilon^n + \alpha\Phi_\varepsilon^n], \nabla\chi) = 0 \quad \forall \chi \in S^h, \tag{2.32b}$$

$$\gamma(\nabla U_\varepsilon^n, \nabla[\chi - U_\varepsilon^n]) \geq (W_\varepsilon^n + \gamma^{-1}U_\varepsilon^{n-1}, \chi - U_\varepsilon^n)^h \quad \forall \chi \in K^h. \tag{2.32c}$$

Note that for $\alpha = 0$, (2.32b,c) collapses to an approximation of (Q) similar to the one considered in [5]. Note also that the solutions no longer depend on ε. As (2.32a,b) are now degenerate, existence of a solution $\{\Phi_\varepsilon^n, U_\varepsilon^n, W_\varepsilon^n\}$ to ($\widetilde{\mathrm{P}}^{h,\tau}$) does not appear to be trivial. However, this can easily be established by splitting the nodes into passive and active sets, see e.g. [6]. Moreover, one can show that U_ε^n is unique, $\Phi_\varepsilon^n(p_j)$ is unique if $(c(U_\varepsilon^{n-1}), \chi_j) > 0$ and $W_\varepsilon^n(p_j)$ is unique if $(\pi^h[b(U_\varepsilon^{n-1})], \chi_j) > 0$. Furthermore, one can establish analogues of the energy estimates (2.25) and (2.26). Of course, for ($\widetilde{\mathrm{P}}^{h,\tau}$) it does not appear possible to establish an analogue of the key energy estimate (2.27) that will be crucial for the convergence analysis in Sect. 3. The practical advantage of ($\widetilde{\mathrm{P}}^{h,\tau}$) is, that now one needs to solve for Φ_ε^n just in the conductor and interfacial regions, $U_\varepsilon^{n-1} > -1$, and for $\{U_\varepsilon^n, W_\varepsilon^n\}$ just in the interfacial region, $|U_\varepsilon^{n-1}| < 1$.

3 Convergence

Let

$$U_\varepsilon(t) := \frac{t - t_{n-1}}{\tau_n}U_\varepsilon^n + \frac{t_n - t}{\tau_n}U_\varepsilon^{n-1} \quad t \in [t_{n-1}, t_n],\ n \geq 1, \tag{3.1a}$$

$$U_\varepsilon^+(t) := U_\varepsilon^n, \qquad U_\varepsilon^-(t) := U_\varepsilon^{n-1} \quad t \in (t_{n-1}, t_n],\ n \geq 1. \tag{3.1b}$$

We note for future reference that

$$U_\varepsilon - U_\varepsilon^\pm = (t - t_n^\pm)\frac{\partial U_\varepsilon}{\partial t} \quad t \in (t_{n-1}, t_n),\ n \geq 1, \tag{3.2}$$

where $t_n^+ := t_n$ and $t_n^- := t_{n-1}$. We introduce also

$$\bar{\tau}(t) := \tau_n \quad t \in (t_{n-1}, t_n],\ n \geq 1. \tag{3.3}$$

Using the above notation, and introducing analogous notation for W_ε^+ and Φ_ε^+, $(\mathrm{P}_\varepsilon^{h,\tau})$ can be restated as: Find $\{\Phi_\varepsilon^+, U_\varepsilon, W_\varepsilon^+\} \in L^\infty(0,T;S^h) \times C([0,T];K^h) \times L^\infty(0,T;S^h)$ such that for all $\chi \in L^\infty(0,T;S^h)$ and $z^h \in L^\infty(0,T;K^h)$

$$\int_0^T (\Lambda_\varepsilon(U_\varepsilon^-)\nabla\Phi_\varepsilon^+, \nabla\chi)\mathrm{d}t + \int_0^T \int_{\partial_\phi\Omega} (\Phi_\varepsilon^+ - g)\chi \,\mathrm{d}s\mathrm{d}t = 0, \tag{3.4a}$$

$$\int_0^T \left[\gamma\left(\frac{\partial U_\varepsilon}{\partial t}, \chi\right)^h + (\Xi_\varepsilon(U_\varepsilon^-)\nabla[W_\varepsilon^+ + \alpha\Phi_\varepsilon^+], \nabla\chi)\right]\mathrm{d}t = 0, \tag{3.4b}$$

$$\gamma\int_0^T (\nabla U_\varepsilon^+, \nabla[z^h - U_\varepsilon^+])\mathrm{d}t \geq \int_0^T (W_\varepsilon^+ + \gamma^{-1}U_\varepsilon^-, z^h - U_\varepsilon^+)^h \mathrm{d}t. \tag{3.4c}$$

Lemma 3.1 *Let $u^0 \in K \cap W^{1,p}(\Omega)$, $p > 3$, with $\fint u^0 \in (-1,1)$. Let $\{\mathcal{T}^h, U_\varepsilon^0, \{\tau_n\}_{n=1}^N, \varepsilon\}_{h>0}$ be such that Ω and $\{\mathcal{T}^h\}_{h>0}$ fulfill assumption* (A), *$\varepsilon \in (0,1)$ with $\varepsilon \to 0$ as $h \to 0$ and $\tau_n \leq C\tau_{n-1} \leq C\varepsilon^2$, $n = 2 \to N$. Then there exist a subsequence of $\{\Phi_\varepsilon^+, U_\varepsilon, W_\varepsilon^+\}_h$, where $\{\Phi_\varepsilon^+, U_\varepsilon, W_\varepsilon^+\}$ solve $(\mathrm{P}_\varepsilon^{h,\tau})$, and a function*

$$u \in L^\infty(0,T;K) \cap H^1(0,T;(H^1(\Omega))') \tag{3.5}$$

with $u(\cdot,0) = u^0(\cdot)$ in $L^2(\Omega)$ and $\fint u(\cdot,t) = \fint u^0$ for a.a. $t \in (0,T)$, such that as $h \to 0$

$$U_\varepsilon, U_\varepsilon^\pm \to u \quad \text{weak-}* \text{ in } L^\infty(0,T;H^1(\Omega)), \tag{3.6a}$$

$$\mathcal{G}\frac{\partial U_\varepsilon}{\partial t} \to \mathcal{G}\frac{\partial u}{\partial t} \quad \text{weakly in } L^2(0,T;H^1(\Omega)), \tag{3.6b}$$

$$U_\varepsilon, U_\varepsilon^\pm \to u \quad \text{strongly in } L^2(0,T;L^s(\Omega)), \tag{3.7a}$$

$$\Xi_\varepsilon(U_\varepsilon^-) \to b(u)\mathcal{I}, \qquad \Lambda_\varepsilon(U_\varepsilon^-) \to c(u)\mathcal{I} \quad \text{strongly in } L^2(0,T;L^s(\Omega)), \tag{3.7b}$$

for all $s \in [2,6]$. If in addition $u^0 \in H^2(\Omega)$ with $\frac{\partial u^0}{\partial \nu} = 0$ on $\partial\Omega$ and

$$\alpha^2 \int_0^T |\pi^h[F_\varepsilon'(U_\varepsilon^-)]|_{0,\partial_\phi\Omega}^2 \mathrm{d}t \leq C, \tag{3.8}$$

then u in addition to (3.5) *satisfies*

$$u \in L^2(0,T;H^2(\Omega)) \tag{3.9}$$

and there exists a subsequence of $\{\Phi_\varepsilon^+, U_\varepsilon, W_\varepsilon^+\}_h$ satisfying (3.6a,b), (3.7a,b) *and as $h \to 0$*

$$\Delta^h U_\varepsilon, \Delta^h U_\varepsilon^\pm \to \Delta u \quad \text{weakly in } L^2(\Omega_T), \tag{3.10a}$$

$$U_\varepsilon, U_\varepsilon^\pm \to u \quad \text{weakly in } L^2(0,T;W^{1,s}(\Omega)), \text{ for any } s \in [2,6], \tag{3.10b}$$

$$U_\varepsilon, U_\varepsilon^\pm \to u \quad \text{strongly in } L^2(0,T;C^{0,\beta}(\overline{\Omega})), \text{ for any } \beta \in \left(0, \frac{1}{2}\right). \tag{3.10c}$$

Finally, on extracting a further subsequence, it holds for a.a. $t \in (0,T)$ that

$$U_\varepsilon^\pm(\cdot,t) \to u(\cdot,t) \quad \text{strongly in } C^{0,\beta}(\overline{\Omega}) \text{ as } h \to 0. \tag{3.10d}$$

Proof The proof largely follows the proof of Lemma 3.1 in BNS. Noting the definitions (3.1a,b), (3.3), the bounds in (2.21), (2.25) and (2.26) together with a Poincaré inequality and (2.31) imply that

$$\begin{aligned}
&\|[\Lambda_\varepsilon(U_\varepsilon^-)]^{\frac{1}{2}}\nabla\Phi_\varepsilon^+\|^2_{L^2(\Omega_T)} + \|\Phi_\varepsilon^+\|^2_{L^2(0,T;L^2(\partial_\phi\Omega))} + \|U_\varepsilon^{(\pm)}\|^2_{L^\infty(0,T;H^1(\Omega))}\\
&\quad + \left\|\bar\tau^{\frac{1}{2}}\frac{\partial U_\varepsilon}{\partial t}\right\|^2_{L^2(0,T;H^1(\Omega))} + \|[\Xi_\varepsilon(U_\varepsilon^-)]^{\frac{1}{2}}\nabla W_\varepsilon^+\|^2_{L^2(\Omega_T)} + \left\|\mathcal{G}\frac{\partial U_\varepsilon}{\partial t}\right\|^2_{L^2(0,T;H^1(\Omega))}\\
&\quad + \tau^{-\frac{1}{2}}\left\|\bar\tau^{\frac{1}{2}}\frac{\partial U_\varepsilon}{\partial t}\right\|^2_{L^2(\Omega_T)} \le C. \qquad (3.11)
\end{aligned}$$

Furthermore, it follows from (3.2) and (3.11) that

$$\|U_\varepsilon - U_\varepsilon^\pm\|^2_{L^2(0,T;H^1(\Omega))} \le \left\|\bar\tau\frac{\partial U_\varepsilon}{\partial t}\right\|^2_{L^2(0,T;H^1(\Omega))} \le C\tau. \qquad (3.12)$$

Hence, on noting (3.11), (3.12), $U_\varepsilon(\cdot,t)\in K^h$, and (1.12a) we can choose a subsequence $\{\Phi_\varepsilon^+, U_\varepsilon, W_\varepsilon^+\}_h$ such that the convergence results (3.5), (3.6a,b) and (3.7a) hold. Moreover, (3.5) and Theorem 2.1 yield, on noting (1.12b) and (2.13) that the subsequence satisfies the additional initial and integral conditions.

We now consider the first result in (3.7b). It holds that

$$\begin{aligned}
&\|b(u)\mathcal{I} - \Xi_\varepsilon(U_\varepsilon^-)\|_{L^2(0,T;L^s(\Omega))} \le \|b(u) - b(U_\varepsilon^-)\|_{L^2(0,T;L^s(\Omega))}\\
&\quad + \|b(U_\varepsilon^-) - b_\varepsilon(U_\varepsilon^-)\|_{L^2(0,T;L^s(\Omega))} + \|b_\varepsilon(U_\varepsilon^-)\mathcal{I} - \Xi_\varepsilon(U_\varepsilon^-)\|_{L^2(0,T;L^s(\Omega))}. \qquad (3.13)
\end{aligned}$$

Noting the Lipschitz continuity of b on $\mathcal{K}$, (2.20b), (2.11) and (3.11), we have that

$$\begin{aligned}
&\|b(u) - b(U_\varepsilon^-)\|_{L^2(0,T;L^s(\Omega))} + \|b_\varepsilon(U_\varepsilon^-)\mathcal{I} - \Xi_\varepsilon(U_\varepsilon^-)\|_{L^2(0,T;L^s(\Omega))}\\
&\quad \le 2\|u - U_\varepsilon^-\|_{L^2(0,T;L^s(\Omega))} + Ch^{(\frac{3}{s}-\frac{1}{2})}\|\nabla U_\varepsilon^-\|_{L^2(\Omega_T)}\\
&\quad \le 2\|u - U_\varepsilon^-\|_{L^2(0,T;L^s(\Omega))} + Ch^{(\frac{3}{s}-\frac{1}{2})}. \qquad (3.14)
\end{aligned}$$

It follows from (2.18b) and (1.5) that

$$\|b(U_\varepsilon^-) - b_\varepsilon(U_\varepsilon^-)\|_{L^2(0,T;L^s(\Omega))} \le Cb_\varepsilon(1) \le C\varepsilon. \qquad (3.15)$$

Combining (3.13), (3.14), (3.15) and noting (3.7a) and our assumptions on ε yields the desired first result (3.7b). A similar argument to the above yields the second result in (3.7b).

We now prove the results (3.10a–c). It follows from (2.1), (2.14), (2.16), (2.12), our assumptions on u^0 and (2.10) that

$$\begin{aligned}
|\Delta^h U_\varepsilon^0|_0^2 &= |\Delta^h(\pi^h u^0)|_0^2 \le |\Delta^h(\pi^h u^0)|_h^2 = -(\nabla(\pi^h u^0), \nabla(\Delta^h(\pi^h u^0)))\\
&= -(\nabla u^0, \nabla(\Delta^h(\pi^h u^0))) + (\nabla(I-\pi^h)u^0, \nabla(\Delta^h(\pi^h u^0)))\\
&\le |\Delta u^0|_0|\Delta^h(\pi^h u^0)|_0 + Ch|u^0|_2|\nabla(\Delta^h(\pi^h u^0))|_0 \le C|u^0|_2^2 \le C. \qquad (3.16)
\end{aligned}$$

Moreover, (2.27), (2.31), (3.16), (2.1), (2.14), (3.1a,b) and our assumptions on $\{\tau_n\}_{n=1}^N$ yield that

$$\|\Delta^h U_\varepsilon^{(\pm)}\|_{L^2(\Omega_T)} \le C. \qquad (3.17)$$

From (3.17), (2.16), (2.13), (2.15), (3.11) and (3.6a) we have for any $\eta \in L^2(0,T;W^{1,q}(\Omega))$, $q>3$, that

$$\begin{aligned}\int_0^T (\Delta^h U_\varepsilon^{(\pm)},\eta)\mathrm{d}t &= \int_0^T (\Delta^h U_\varepsilon^{(\pm)},(I-\pi^h)\eta)\mathrm{d}t\\ &\quad+\int_0^T \left[(\Delta^h U_\varepsilon^{(\pm)},\pi^h\eta)-(\Delta^h U_\varepsilon^{(\pm)},\pi^h\eta)^h\right]\mathrm{d}t\\ &\quad+\int_0^T (\nabla U_\varepsilon^{(\pm)},\nabla(I-\pi^h)\eta)\mathrm{d}t-\int_0^T (\nabla U_\varepsilon^{(\pm)},\nabla\eta)\mathrm{d}t\\ &\to -\int_0^T (\nabla u,\nabla\eta)\mathrm{d}t \quad \text{as } h\to 0. \end{aligned} \tag{3.18}$$

Combining (3.17), (3.18) and the denseness of $L^2(0,T;W^{1,q}(\Omega))$ in $L^2(\Omega_T)$ yields (3.10a) and, in particular, $\Delta u \in L^2(\Omega_T)$. This together with elliptic regularity, as Ω is a prism, and (3.5) proves (3.9). Furthermore, it follows from (3.10a) and (2.17) that (3.10b) holds on extracting a further subsequence. In addition, the result on U_ε in (3.10c) follows from (3.10b), (3.6b), (1.12a) and the compact embedding $W^{1,s}(\Omega)\hookrightarrow C^{0,\beta}(\overline{\Omega})$.

We now establish (3.10c) for $U_\varepsilon^\pm$, using a technique from [10]. For any $\beta\in(0,\frac{1}{2})$, $s\in(\frac{3}{1-\beta},6]$ and any $\bar{s}\in(\frac{3}{1-\beta},s)$ it holds on noting the compact embedding $W^{1,\bar{s}}(\Omega)\hookrightarrow C^{0,\beta}(\overline{\Omega})$, (3.12) and (3.10b) that

$$\begin{aligned}&\|U_\varepsilon-U_\varepsilon^\pm\|_{L^2(0,T;C^{0,\beta}(\overline{\Omega}))}\\ &\quad\le \|U_\varepsilon-U_\varepsilon^\pm\|_{L^2(0,T;W^{1,\bar{s}}(\Omega))}\\ &\quad\le \|U_\varepsilon-U_\varepsilon^\pm\|^q_{L^2(0,T;H^1(\Omega))}\|U_\varepsilon-U_\varepsilon^\pm\|^{1-q}_{L^2(0,T;W^{1,s}(\Omega))}\le C\tau^{\frac{q}{2}}, \end{aligned} \tag{3.19}$$

where $q=\frac{2(s-\bar{s})}{(s-2)\bar{s}}\in(0,1)$. Combining (3.19), assumption (ii) and the established result on U_ε in (3.10c) yields the desired result on $U_\varepsilon^\pm$ in (3.10c). Finally, the desired result (3.10d) follows immediately from (3.10c). □

Remark 3.1 We note that the necessary assumption (3.8) trivially holds if $\alpha=0$. Moreover, when $\alpha>0$ it holds if e.g. $U_\varepsilon(x,t)=1$ for all $x\in\partial_\phi\Omega$ and $t\in[0,T]$, and this condition held in all our numerical experiments provided $u^0=1$ on $\partial_\phi\Omega$ and either L_1 is chosen sufficiently large or T is chosen sufficiently small. This can be made rigorous for the approximation ($\widetilde{\mathrm{P}}^{h,\tau}$), see Remark 2.2, as the degeneracy in (2.32b) leads to finite speed of propagation of the numerical interfacial region; at each time level it can move locally at most one mesh point, see [6]. We note furthermore that in order to establish the result on $U_\varepsilon^\pm$ in (3.10c), we did not have to assume a uniform time step size. This is an improvement on the result derived in BNS. The same holds true for our main convergence result, see Theorem 3.1 below.

From (3.11), (2.19a,b), (2.18a,b), (1.5) and (3.10d) we see that we can control $\nabla\Phi_\varepsilon^+$ and ∇W_ε^+ on the sets where $\Lambda_\varepsilon(U_\varepsilon^-)$ and $\Xi_\varepsilon(U_\varepsilon^-)$ are bounded below independently of ε, and hence h, i.e. on the sets where $u>-1$ and $|u|<1$, respectively. It is therefore possible to prove convergence of the terms $\Lambda_\varepsilon(U_\varepsilon^-)\nabla\Phi_\varepsilon^+$, $\Xi_\varepsilon(U_\varepsilon^-)\nabla\Phi_\varepsilon^+$ and $\Xi_\varepsilon(U_\varepsilon^-)\nabla W_\varepsilon^+$ in (3.4a–c) to their respective expected limits.

Lemma 3.2 *Let all the assumptions of Lemma 3.1 hold. Then for a.a. $t \in (0,T)$ there exist functions*

$$\begin{aligned} &\phi(\cdot,t) \in H^1_{loc}(\{u(\cdot,t) > -1\}),\\ &w(\cdot,t) \equiv -\gamma\Delta u(\cdot,t) - \gamma^{-1}u(\cdot,t) \in H^1_{loc}(\{|u(\cdot,t)| < 1\}); \end{aligned} \tag{3.20}$$

where $\{u(\cdot,t) > -1\} := \{x \in \Omega : u(x,t) > -1\}$ and $\{|u(\cdot,t)| < 1\} := \{x \in \Omega : |u(x,t)| < 1\}$. Moreover, on assuming that

$$u(x,t) = 1 \quad \forall x \in \partial_\phi\Omega, \text{ for a.a. } t \in (0,T), \tag{3.21}$$

and extracting a further subsequence from the subsequence $\{\Phi_\varepsilon^+, U_\varepsilon, W_\varepsilon^+\}_h$ in Lemma 3.1, it holds as $h \to 0$ that

$$\Phi_\varepsilon^+ \to \phi \quad \text{weakly in } L^2(0,T;L^2(\partial_\phi\Omega)), \tag{3.22a}$$

$$\Lambda_\varepsilon(U_\varepsilon^-)\nabla\Phi_\varepsilon^+ \to \mathcal{H}_{\{u>-1\}}c(u)\nabla\phi \quad \text{weakly in } L^2(\Omega_T), \tag{3.22b}$$

$$\Xi_\varepsilon(U_\varepsilon^-)\nabla\Phi_\varepsilon^+ \to \mathcal{H}_{\{|u|<1\}}b(u)\nabla\phi \quad \text{weakly in } L^2(\Omega_T), \tag{3.22c}$$

$$\Xi_\varepsilon(U_\varepsilon^-)\nabla W_\varepsilon^+ \to \mathcal{H}_{\{|u|<1\}}b(u)\nabla w \quad \text{weakly in } L^2(\Omega_T); \tag{3.22d}$$

where $\mathcal{H}_{\{u>-1\}}$ and $\mathcal{H}_{\{|u|<1\}}$ are the characteristic functions of the sets $\{u > -1\} := \{(x,t) \in \Omega_T : u(x,t) > -1\}$ and $\{|u| < 1\} := \{(x,t) \in \Omega_T : |u(x,t)| < 1\}$, respectively.

Proof See the proof of Lemma 3.4 in BNS, which immediately carries over to three space dimensions. □

Theorem 3.1 *Let the assumptions of Lemma 3.2 hold. Then there exists a subsequence of $\{\Phi_\varepsilon^+, U_\varepsilon, W_\varepsilon^+\}_h$, where $\{\Phi_\varepsilon^+, U_\varepsilon, W_\varepsilon^+\}$ solve $(\mathrm{P}_\varepsilon^{h,\tau})$, and functions $\{\phi, u, w\}$ satisfying (3.5), (3.9) and (3.20). In addition, as $h \to 0$ the following hold*: (3.6a,b), (3.7a,b), (3.10a–d) *and* (3.22a–d). *Furthermore, we have that $\{\phi, u, w\}$ fulfill $u(\cdot,0) = u^0(\cdot)$ in $L^2(\Omega)$ and satisfy for all $\eta \in L^2(0,T;H^1(\Omega))$*

$$\int_{\{u>-1\}} c(u)\nabla\phi.\nabla\eta \mathrm{d}x\mathrm{d}t + \int_0^T \int_{\partial_\phi\Omega} (\phi - g)\eta \mathrm{d}s\mathrm{d}t = 0, \tag{3.23a}$$

$$\gamma \int_0^T \left\langle \frac{\partial u}{\partial t}, \eta \right\rangle \mathrm{d}t + \int_{\{|u|<1\}} b(u)\nabla[w + \alpha\phi].\nabla\eta \mathrm{d}x\mathrm{d}t = 0; \tag{3.23b}$$

where $w(\cdot,t) \equiv -\gamma\Delta u(\cdot,t) - \gamma^{-1}u(\cdot,t)$ on the set $\{|u(\cdot,t)| < 1\}$ for a.a. $t \in (0,T)$.

Proof The proof is a straightforward adaption of the proof to Theorem 3.6 in BNS to three space dimensions. As we will later appeal to a density argument, we choose $\chi \equiv \pi^h\eta$ in (3.4a,b) for a $\eta \in H^1(0,T;H^2(\Omega))$ and analyse the subsequent terms. It follows from (2.15), the embedding $H^1(0,T;X) \hookrightarrow C([0,T];X)$, (3.11) and (2.12) that

$$\left| \int_0^T \left[\left(\frac{\partial U_\varepsilon}{\partial t}, \pi^h\eta \right)^h - \left(\frac{\partial U_\varepsilon}{\partial t}, \pi^h\eta \right) \right] \mathrm{d}t \right|$$

$$= \left| - \int_0^T \left(U_\varepsilon, \frac{\partial(\pi^h \eta)}{\partial t} \right)^h \mathrm{d}t + (U_\varepsilon(\cdot, T), \pi^h \eta(\cdot, T))^h - (U_\varepsilon(\cdot, 0), \pi^h \eta(\cdot, 0))^h \right.$$

$$\left. + \int_0^T \left(U_\varepsilon, \frac{\partial(\pi^h \eta)}{\partial t} \right) \mathrm{d}t - (U_\varepsilon(\cdot, T), \pi^h \eta(\cdot, T)) + (U_\varepsilon(\cdot, 0), \pi^h \eta(\cdot, 0)) \right|$$

$$\leq Ch \|U_\varepsilon\|_{L^\infty(0,T;L^2(\Omega))} \|\pi^h \eta\|_{H^1(0,T;H^1(\Omega))} \leq Ch \|\eta\|_{H^1(0,T;H^2(\Omega))}. \tag{3.24}$$

Moreover, combining (1.13), (3.11) and (2.12) yields that

$$\left| \int_0^T \left(\frac{\partial U_\varepsilon}{\partial t}, (I - \pi^h)\eta \right) \mathrm{d}t \right| \leq C \|\mathcal{G} \frac{\partial U_\varepsilon}{\partial t}\|_{L^2(0,T;H^1(\Omega))} \|(I - \pi^h)\eta\|_{L^2(0,T;H^1(\Omega))}$$

$$\leq Ch \|\eta\|_{L^2(0,T;H^2(\Omega))}. \tag{3.25}$$

Hence it follows from (3.24), (3.25) and (3.6b) that

$$\int_0^T \left(\frac{\partial U_\varepsilon}{\partial t}, \pi^h \eta \right)^h \mathrm{d}t \to \int_0^T \left\langle \frac{\partial u}{\partial t}, \eta \right\rangle \mathrm{d}t \quad \text{as } h \to 0. \tag{3.26}$$

In addition, it holds on noting (3.11), g as in (1.8), a trace inequality and (2.12) that

$$\left| \int_0^T \int_{\partial_\phi \Omega} (\Phi_\varepsilon^+ - g)(I - \pi^h)\eta \mathrm{d}s\mathrm{d}t \right|$$

$$\leq \left[\|\Phi_\varepsilon^+\|_{L^2(0,T;L^2(\partial_\phi\Omega))} + \|g\|_{L^2(0,T;L^2(\partial_\phi\Omega))} \right] \|(I - \pi^h)\eta\|_{L^2(0,T;L^2(\partial_\phi\Omega))}$$

$$\leq C \|(I - \pi^h)\eta\|_{L^2(0,T;H^1(\Omega))} \leq Ch \|\eta\|_{L^2(0,T;H^2(\Omega))}. \tag{3.27}$$

In view of (2.19a–c), (3.11) and (2.12) we deduce that

$$\left| \int_0^T (\Xi_\varepsilon(U_\varepsilon^-) \nabla W_\varepsilon^+, \nabla(I - \pi^h)\eta) \mathrm{d}t \right|$$

$$\leq \|\Xi_\varepsilon(U_\varepsilon^-) \nabla W_\varepsilon^+\|_{L^2(\Omega_T)} \|(I - \pi^h)\eta\|_{L^2(0,T;H^1(\Omega))}$$

$$\leq \|[\Xi_\varepsilon(U_\varepsilon^-)]^{\frac{1}{2}} \nabla W_\varepsilon^+\|_{L^2(\Omega_T)} \|(I - \pi^h)\eta\|_{L^2(0,T;H^1(\Omega))}$$

$$\leq Ch \|\eta\|_{L^2(0,T;H^2(\Omega))} \tag{3.28a}$$

and similarly

$$\left| \int_0^T (\Lambda_\varepsilon(U_\varepsilon^-) \nabla \Phi_\varepsilon^+, \nabla(I - \pi^h)\eta) \mathrm{d}t \right| + \left| \int_0^T (\Xi_\varepsilon(U_\varepsilon^-) \nabla \Phi_\varepsilon^+, \nabla(I - \pi^h)\eta) \mathrm{d}t \right|$$

$$\leq C \|(I - \pi^h)\eta\|_{L^2(0,T;H^1(\Omega))} \leq Ch \|\eta\|_{L^2(0,T;H^2(\Omega))}. \tag{3.28b}$$

Combining (3.28a,b) and (3.22b–d) yields that as $h \to 0$

$$\int_0^T (\Lambda_\varepsilon(U_\varepsilon^-) \nabla \Phi_\varepsilon^+, \nabla(\pi^h \eta)) \mathrm{d}t \to \int_{\{u > -1\}} c(u) \nabla \phi . \nabla \eta \mathrm{d}x \mathrm{d}t, \tag{3.29a}$$

$$\int_0^T (\Xi_\varepsilon(U_\varepsilon^-)\nabla\Phi_\varepsilon^+, \nabla(\pi^h\eta))\mathrm{d}t \to \int_{\{|u|<1\}} b(u)\nabla\phi.\nabla\eta\mathrm{d}x\mathrm{d}t, \tag{3.29b}$$

$$\int_0^T (\Xi_\varepsilon(U_\varepsilon^-)\nabla W_\varepsilon^+, \nabla(\pi^h\eta))\mathrm{d}t \to \int_{\{|u|<1\}} b(u)\nabla w.\nabla\eta\mathrm{d}x\mathrm{d}t. \tag{3.29c}$$

Finally, it follows from (3.4a,b), (3.26), (3.27), (3.22a), (3.29a–c) and the denseness of $H^1(0,T;\ H^2(\Omega))$ in $L^2(0,T;H^1(\Omega))$ that the desired results (3.23a,b) hold, on recalling (3.5) and (3.20). □

4 Solution of the Discrete System

We now discuss algorithms for solving the resulting system of algebraic equations for $\{\Phi_\varepsilon^n, U_\varepsilon^n, W_\varepsilon^n\}$ arising at each time level from the approximation $(\mathrm{P}_\varepsilon^{h,\tau})$.

As (2.9a) in $(\mathrm{P}_\varepsilon^{h,\tau})$ is independent of $\{U_\varepsilon^n, W_\varepsilon^n\}$, we solve it first to obtain Φ_ε^n; then solve (2.9b,c) for $\{U_\varepsilon^n, W_\varepsilon^n\}$. The solution of (2.9a) is straightforward, as it is a linear equation.

Adopting the obvious notation, the system (2.9b,c) can be rewritten as: Find $\{\underline{U}_\varepsilon^n, \underline{W}_\varepsilon^n\} \in \mathcal{K}^{\mathcal{J}} \times \mathbb{R}^{\mathcal{J}}$, where $\mathcal{J} := \#J$, such that

$$\gamma M\underline{U}_\varepsilon^n + \tau_n A^{n-1}\underline{W}_\varepsilon^n = \underline{r} \tag{4.1a}$$

$$\gamma(\underline{V} - \underline{U}_\varepsilon^n)^T B\underline{U}_\varepsilon^n - (\underline{V} - \underline{U}_\varepsilon^n)^T M\underline{W}_\varepsilon^n \geq (\underline{V} - \underline{U}_\varepsilon^n)^T \underline{s} \quad \forall \underline{V} \in \mathcal{K}^{\mathcal{J}}, \tag{4.1b}$$

where M, B and A^{n-1} are symmetric $\mathcal{J} \times \mathcal{J}$ matrices with entries

$$M_{ij} := (\chi_i, \chi_j)^h, \qquad B_{ij} := (\nabla\chi_i, \nabla\chi_j), \qquad A_{ij}^{n-1} := (\Xi_\varepsilon(U_\varepsilon^{n-1})\nabla\chi_i, \nabla\chi_j)$$

and

$$\underline{r} := \gamma M\underline{U}_\varepsilon^{n-1} - \alpha\tau_n A^{n-1}\underline{\Phi}_\varepsilon^n \in \mathbb{R}^{\mathcal{J}}, \qquad \underline{s} := \gamma^{-1} M\underline{U}_\varepsilon^{n-1} \in \mathbb{R}^{\mathcal{J}}.$$

In this paper, we will consider two solutions methods for the above system of algebraic equations: a block Gauss–Seidel scheme from BNS and a Uzawa-multigrid method based on the solver in [21]. However, we note that very recently in [1] the authors proposed a fully nonlinear multigrid method that can be directly applied to (4.1a,b).

4.1 Block Gauss–Seidel Scheme

We recall the following block "Gauss–Seidel type" iterative method to solve (2.9b,c) from BNS. On letting $A^{n-1} \equiv A_D - A_L - A_L^T$, with A_L and A_D being the lower triangular and diagonal parts of the matrix A^{n-1}, similarly for B, the method can be formulated as follows.

Given $\{U_\varepsilon^{n,0}, W_\varepsilon^{n,0}\} \in K^h \times S^h$, for $k \geq 1$ find $\{U_\varepsilon^{n,k}, W_\varepsilon^{n,k}\} \in K^h \times S^h$ such that

$$\gamma M\underline{U}_\varepsilon^{n,k} + \tau_n(A_D - A_L)\underline{W}_\varepsilon^{n,k} = \underline{r} + \tau_n A_L^T \underline{W}_\varepsilon^{n,k-1} \tag{4.2a}$$

$$(\underline{V} - \underline{U}_\varepsilon^{n,k})^T(\gamma(B_D - B_L)\underline{U}_\varepsilon^{n,k} - M\underline{W}_\varepsilon^{n,k}) \geq (\underline{V} - \underline{U}_\varepsilon^{n,k})^T(\underline{s} + \gamma B_L^T \underline{U}_\varepsilon^{n,k-1}) \quad \forall \underline{V} \in \mathcal{K}^{\mathcal{J}}. \tag{4.2b}$$

It is possible to prove convergence of the iterative method (4.1a,b) to the solution of the nonlinear system (2.9b,c), see Theorem 4.1 in BNS.

Remark 4.1 We note that (4.2a,b) can be solved explicitly for $j = 1 \to \mathcal{J}$. In particular, let $\hat{\underline{r}} := \underline{r} + \tau_n (A_L \underline{W}_\varepsilon^{n,k} + A_L^T \underline{W}_\varepsilon^{n,k-1})$ and $\hat{\underline{s}} := \underline{s} + \gamma (B_L \underline{U}_\varepsilon^{n,k} + B_L^T \underline{U}_\varepsilon^{n,k-1})$. Then, for $|A_{jj}^{n-1}| > 0$, on recalling (1.14), we set for $j = 1 \to \mathcal{J}$

$$[\underline{U}_\varepsilon^{n,k}]_j = \left[\frac{M_{jj} \hat{\underline{r}}_j + \tau_n A_{jj}^{n-1} \hat{\underline{s}}_j}{\gamma [M_{jj}]^2 + \tau_n \gamma A_{jj}^{n-1} B_{jj}} \right]_{\mathcal{K}} \quad \text{and} \quad [\underline{W}_\varepsilon^{n,k}]_j = \frac{\hat{\underline{r}}_j - \gamma M_{jj} [\underline{U}_\varepsilon^{n,k}]_j}{\tau_n A_{jj}^{n-1}}. \tag{4.3}$$

Remark 4.2 For the approximation $(\widetilde{\mathrm{P}}^{h,\tau})$, see Remark 2.2, we have that $A_{jj}^{n-1} = 0$ for $j \in J_{deg} := \{ j \in J : \pi^h [b(U_\varepsilon^{n-1})] \equiv 0 \text{ on } \mathrm{supp}(\chi_j) \}$. For those j, one needs to replace (4.3) with $[\underline{U}_\varepsilon^{n,k}]_j = [\underline{U}_\varepsilon^{n-1}]_j$ and $[\underline{W}_\varepsilon^{n,k}]_j$ can be chosen arbitrarily, where for computational purposes we set $[\underline{W}_\varepsilon^{n,k}]_j = [\underline{W}_\varepsilon^{n-1}]_j$.

4.2 Uzawa-Multigrid Algorithm

Uzawa-type algorithms are widely used for the solution of saddle point problems which arise in the constrained minimization of convex functionals or in the discretization of Stokes problems, see e.g. [19] for more details. Very recently, a Uzawa-type iterative solver for a finite element discretization of the Cahn–Hilliard equation with constant mobility, i.e. (Q_γ) with $b(s) \equiv 1$, has been proposed in [21]. They consider a discrete saddle point problem that is equivalent to the discrete constrained minimization problem formulation introduced in [12]. The authors in [21] then propose a preconditioned Uzawa-type algorithm as an efficient solution method for the introduced saddle point problem. Here we will adopt these ideas in order to introduce new iterative schemes for the solution of our approximations (2.9b,c) and (2.32b,c) to the degenerate Cahn–Hilliard equation in (P_γ).

For a given time step n, a preconditioned Uzawa iteration for the system (4.1a,b) can be formulated as follows, see e.g. [20].
Given $W_\varepsilon^{n,0} \in S^h$, for $k \geq 1$ find $\{U_\varepsilon^{n,k}, W_\varepsilon^{n,k}\} \in K^h \times S^h$ such that

$$\gamma (\underline{V} - \underline{U}_\varepsilon^{n,k})^T B \underline{U}_\varepsilon^{n,k} \geq (\underline{V} - \underline{U}_\varepsilon^{n,k})^T \underline{s} + (\underline{V} - \underline{U}_\varepsilon^{n,k})^T M \underline{W}_\varepsilon^{n,k-1} \quad \forall \underline{V} \in \mathcal{K}^{\mathcal{J}}, \tag{4.4a}$$

$$\underline{W}_\varepsilon^{n,k} = \underline{W}_\varepsilon^{n,k-1} + S^{-1} \left(-\gamma M \underline{U}_\varepsilon^{n,k} - \tau_n A^{n-1} \underline{W}_\varepsilon^{n,k-1} + \underline{r} \right); \tag{4.4b}$$

where $S : \mathbb{R}^{\mathcal{J}} \to \mathbb{R}^{\mathcal{J}}$ is a suitably chosen preconditioner.

We follow [21] for the choice of the preconditioner S. It is motivated by the fact that once we know the solution $\underline{U}_\varepsilon^n$ on the coincidence set

$$\hat{J}(\underline{U}_\varepsilon^n) = \left\{ j \in J : \left| [\underline{U}_\varepsilon^n]_j \right| = 1 \right\},$$

the problem (4.1a,b) is reduced to a linear system of the form

$$\begin{pmatrix} \gamma \hat{B}(\underline{U}_\varepsilon^n) & -\hat{M}(\underline{U}_\varepsilon^n) \\ \gamma M & \tau_n A^{n-1} \end{pmatrix} \begin{pmatrix} \underline{U}_\varepsilon^n \\ \underline{W}_\varepsilon^n \end{pmatrix} = \begin{pmatrix} \hat{s}(\underline{U}_\varepsilon^n) \\ \underline{r} \end{pmatrix}. \tag{4.5}$$

Here, the matrices $\hat{B}$, $\hat{M}$ and the right hand side $\hat{s}$ depend only on the coincidence set $\hat{J}(\underline{U}_\varepsilon^n)$ and the values of $\underline{U}_\varepsilon^n$ on it, and are given by

$$\hat{B}_{ij} = \begin{cases} \delta_{ij} & i \in \hat{J} \\ B_{ij} & \text{else,} \end{cases} \qquad \hat{M}_{ij} = \begin{cases} 0 & i \in \hat{J} \\ M_{ij} & \text{else,} \end{cases} \quad j \in J, \tag{4.6a}$$

and

$$\hat{s}_i = \begin{cases} \gamma[\underline{U}_\varepsilon^n]_i & i \in \hat{J} \\ s_i & \text{else.} \end{cases} \tag{4.6b}$$

Applying a Schur complement approach, the system (4.5) can be reduced to $S(\underline{U}_\varepsilon^n)\underline{W}_\varepsilon^n = -M\hat{B}(\underline{U}_\varepsilon^n)^{-1}\hat{s}(\underline{U}_\varepsilon^n) + \underline{r}$, where $S(\underline{U}_\varepsilon^n) = M\hat{B}(\underline{U}_\varepsilon^n)^{-1}\hat{M}(\underline{U}_\varepsilon^n) + \tau_n A^{n-1}$ is the Schur complement of (4.5).

As $S(\underline{U}_\varepsilon^n)$ is unknown in practice, we approximate the solution $\underline{U}_\varepsilon^n$ with the solution $\underline{U}_\varepsilon^{n,k}$ from the first Uzawa step (4.4a), and then use the preconditioner

$$S = S(\underline{U}_\varepsilon^{n,k}) = M\hat{B}(\underline{U}_\varepsilon^{n,k})^{-1}\hat{M}(\underline{U}_\varepsilon^{n,k}) + \tau_n A^{n-1}$$

in the second Uzawa step (4.4b). With this choice of preconditioner, on noting that (4.4a) implies that $\gamma\hat{B}(\underline{U}_\varepsilon^{n,k})\underline{U}_\varepsilon^{n,k} - \hat{M}(\underline{U}_\varepsilon^{n,k})\underline{W}_\varepsilon^{n,k-1} = \hat{s}(\underline{U}_\varepsilon^{n,k})$, the iteration (4.4a,b) can be equivalently formulated as

$$\gamma(\underline{V} - \underline{U}_\varepsilon^{n,k})^T B\underline{U}_\varepsilon^{n,k} \geq (\underline{V} - \underline{U}_\varepsilon^{n,k})^T \underline{s} + (\underline{V} - \underline{U}_\varepsilon^{n,k})^T M\underline{W}_\varepsilon^{n,k-1} \quad \forall \underline{V} \in \mathcal{K}^{\mathcal{J}}, \tag{4.7a}$$

$$\underline{W}_\varepsilon^{n,k} = S(\underline{U}_\varepsilon^{n,k})^{-1}\left(-M\hat{B}(\underline{U}_\varepsilon^{n,k})^{-1}\hat{s}(\underline{U}_\varepsilon^{n,k}) + \underline{r}\right). \tag{4.7b}$$

We note that apart from the structure of the matrix A^{n-1}, our approach (4.7a,b) differs from the one in [21], in that there a term of the form $\gamma(\chi_i, 1)(\chi_j, 1)$ is added to the matrix B in order to better control the mass constraint $(U_\varepsilon^n, 1)^h = (U_\varepsilon^0, 1)^h$. However, in practice we observed no disadvantages when using (4.7a,b).

4.2.1 Solution of the Subproblems

As (4.7a) is independent of $\underline{W}_\varepsilon^{n,k}$, we first solve it to obtain $\underline{U}_\varepsilon^{n,k}$; then solve (4.7b) for $\underline{W}_\varepsilon^{n,k}$. Solving (4.7a) requires the solution of an elliptic variational inequality with a double obstacle. This can be solved by a projected Gauss–Seidel method (PGS) for obstacle problems, i.e. a scalar analogue of the block iteration (4.2a,b), or by a monotone multigrid method (MMG), see [23]. In the second sub-step, (4.7b), of the Uzawa iteration only the coincidence set $\hat{J}^k \equiv \hat{J}(\underline{U}_\varepsilon^{n,k})$ and the values of $\underline{U}_\varepsilon^{n,k}$ on $\hat{J}^k$ are needed in order to compute $\underline{W}_\varepsilon^{n,k}$. Hence, we can stop the iteration for (4.7a) after the coincidence set $\hat{J}^k$ is detected. This usually requires only a few iterations of either PGS or MMG.

Solving (4.7b) is equivalent to solving the linear system

$$\begin{pmatrix} \gamma\hat{B}(\underline{U}_\varepsilon^{n,k}) & -\hat{M}(\underline{U}_\varepsilon^{n,k}) \\ \gamma M & \tau_n A^{n-1} \end{pmatrix} \begin{pmatrix} \widetilde{\underline{U}}^k \\ \underline{W}_\varepsilon^{n,k} \end{pmatrix} = \begin{pmatrix} \hat{s}(\underline{U}_\varepsilon^{n,k}) \\ \underline{r} \end{pmatrix} \tag{4.8}$$

with an auxiliary variable $\widetilde{\underline{U}}^k$, which has fixed values $\widetilde{\underline{U}}^k = \underline{U}_\varepsilon^{n,k}$ on $\hat{J}^k$. Here $\hat{B}$, $\hat{M}$ and $\hat{s}$ are defined analogously to (4.6a,b). As (4.8) is linear, it would be desirable to solve it with a multigrid method. Therefore, we transform (4.8) to the following symmetric system.

$$\begin{pmatrix} \gamma^2\widetilde{B} & -\gamma\hat{M}(\underline{U}_\varepsilon^{n,k}) \\ -\gamma\hat{M}(\underline{U}_\varepsilon^{n,k}) & -\tau_n A^{n-1} \end{pmatrix} \begin{pmatrix} \widetilde{\underline{U}}^k \\ \underline{W}_\varepsilon^{n,k} \end{pmatrix} = \begin{pmatrix} \gamma\widetilde{s} \\ -\widetilde{r} \end{pmatrix}. \tag{4.9}$$

Here the symmetric matrix $\widetilde{B}$ is defined as

$$\widetilde{B}_{ij} = \begin{cases} \delta_{ij} & i \in \hat{J}^k \text{ or } j \in \hat{J}^k \\ \hat{B}_{ij}(\underline{U}_\varepsilon^{n,k}) & \text{else,} \end{cases}$$

while the modified right hand sides $\widetilde{r}$ and $\widetilde{s}$ are defined as

$$\widetilde{s}_i = \begin{cases} \hat{s}_i(\underline{U}_\varepsilon^{n,k}) - \gamma \sum_{j \in \hat{J}^k} \hat{B}_{ij} \left[\underline{U}_\varepsilon^{n,k}\right]_j & i \notin \hat{J}^k \\ \hat{s}_j(\underline{U}_\varepsilon^{n,k}) & \text{else,} \end{cases} \qquad \widetilde{r}_i = \begin{cases} r_i - \gamma M_{ii} \left[\underline{U}_\varepsilon^{n,k}\right]_i & i \in \hat{J}^k \\ r_i & \text{else.} \end{cases}$$

The system (4.9) can be solved by a multigrid method for linear symmetric saddle point problems, see e.g. [31], where convergence for a multigrid method employing a Jacobi smoother is shown. Moreover, the convergence of a large class of block Gauss–Seidel smoothers for saddle-point problems arising from the discretizations of Stokes and Navier–Stokes equations has recently been shown in [25]. We solved the system (4.9) by a multigrid method with block Gauss–Seidel smoother and canonical restriction and prolongation. Our smoother is the linear analogue of the algorithm (4.2a,b), i.e. the variational inequality (4.2b) is replaced by an equality. As the restrictions of the diagonal matrix $\hat{M}$ to the lower grid levels are no longer diagonal, the smoother for the lower grids is appropriately modified. We note that the symmetric structure of (4.9) is crucial for the convergence of the multigrid solver.

Remark 4.3 When using the approximation $(\widetilde{\mathrm{P}}^{h,\tau})$, the system (4.9) is modified as follows, as now the matrix A^{n-1} can have zero entries on the diagonal, see Remark 4.2. Therefore, we will adapt (4.9) slightly, in order to be able to apply a standard smoother in the multigrid solver. To this end, the first step (4.7a) is modified in such a way, that $[\underline{U}_\varepsilon^{n,k}]_i = [\underline{U}_\varepsilon^{n-1}]_i$ for all $i \in J_{deg}$, recall Remark 4.2. This is a very natural modification, as we know that $[\underline{U}_\varepsilon^{n}]_i = [\underline{U}_\varepsilon^{n-1}]_i$ for all $i \in J_{deg}$. Moreover, on noting Remark 3.1, this ensures that $J_{deg} \subset \hat{J}^k$. This allows us to equivalently formulate (4.9) as

$$\begin{pmatrix} \gamma^2 \widetilde{B} & -\gamma \hat{M} \\ -\gamma \hat{M} & -\tau_n A_{deg}^{n-1} \end{pmatrix} \begin{pmatrix} \underline{\widetilde{U}}^k \\ \underline{\widetilde{W}}^k \end{pmatrix} = \begin{pmatrix} \gamma \widetilde{s} \\ -\widetilde{r}_{deg} \end{pmatrix}, \tag{4.10}$$

with another auxiliary variable $\underline{\widetilde{W}}^k$, which has fixed values $[\underline{\widetilde{W}}^k]_j = [\underline{W}_\varepsilon^{n-1}]_j$ for $j \in J_{deg}$. Here the matrix A_{deg}^{n-1} is defined as

$$[A_{deg}^{n-1}]_{ij} = \begin{cases} \delta_{ij} & i \in J_{deg} \text{ or } j \in J_{deg} \\ A_{ij}^{n-1} & \text{else.} \end{cases}$$

The modified right-hand side $\widetilde{r}_{deg}$ is defined as

$$[\widetilde{r}_{deg}]_j = \begin{cases} \tau_n \left[W_\varepsilon^{n-1}\right]_j & j \in J_{deg} \\ \widetilde{r}_j & \text{else,} \end{cases}$$

where we note that $A_{ij}^{n-1} = 0$ if $i \in J_{deg}$ or $j \in J_{deg}$. The new matrix A_{deg}^{n-1} has only positive diagonal entries, and so the system (4.10) can be solved in the same way as (4.9), i.e. with a multigrid solver for linear symmetric saddle point problems with a standard block Gauss–Seidel smoother. Naturally, we set $\underline{W}_\varepsilon^{n,k} := \underline{\widetilde{W}}^k$.

Finally, we note that alternatively, one could employ a suitably adapted smoother directly for the system (4.9), with the matrix A^{n-1} being singular, see e.g. [1].

The full Uzawa-multigrid algorithm for solving (4.1a,b) can then be summarized as follows.

1. Initialization: Start with the initial guess $\underline{U}_\varepsilon^{n,0} = \underline{U}_\varepsilon^{n-1}$, set $\hat{J}^0 = \hat{J}(\underline{U}_\varepsilon^{n,0})$ and compute $\underline{W}_\varepsilon^{n,0}$ by solving the system (4.9) with coincidence set $\hat{J}^0$.
2. Uzawa iterations: for $k = 1, \dots$ do
   - Compute the approximate coincidence set $\hat{J}^k = \hat{J}(\underline{U}_\varepsilon^{n,k})$, where $\underline{U}_\varepsilon^{n,k}$ is obtained from (4.7a) by PGS or MMG (here the iterations are terminated as soon as the coincidence sets for two successive PGS/MMG iterates are the same).
   - If $\hat{J}^k = \hat{J}^{k-1}$ go to step 3.
   - Solve the system (4.9) by the multigrid method with block Gauss–Seidel smoother to obtain $\underline{W}_\varepsilon^{n,k}$.
   - If $\max_{j\in J} |[\underline{W}_\varepsilon^{n,k}]_j - [\underline{W}_\varepsilon^{n,k-1}]_j| < tol$, with tol being the prescribed tolerance, go to step 3.
3. Uzawa iterations have converged: Compute $\underline{U}_\varepsilon^{n,k+1}$ up to the desired accuracy from (4.7a) using $\underline{W}_\varepsilon^{n,k}$.
4. Set $\underline{U}_\varepsilon^{n} = \underline{U}_\varepsilon^{n,k+1}$, $\underline{W}_\varepsilon^{n} = \underline{W}_\varepsilon^{n,k}$.

5 Numerical Results

In order to define the initial shape of the void we introduce the following function. Given $z \in \mathbb{R}^3$, $a \in \mathbb{R}^3$ with $\min\{a_1, a_2, a_3\} = 1$ and $R \in \mathbb{R}_{>0}$ we define

$$v(z, a, R; x) := \begin{cases} -1 & r(z, a; x) - R \le -\dfrac{\gamma\pi}{2} \\ \sin\left(\dfrac{r(z, a; x) - R}{\gamma}\right) & |r(z, a; x) - R| < \dfrac{\gamma\pi}{2} \\ 1 & r(z, a; x) - R \ge \dfrac{\gamma\pi}{2}, \end{cases} \tag{5.1}$$

where $(r(z, a; x) - R)$ denotes a suitable distance function for a ball with radius R, a prism with dimensions $a_1 R \times a_2 R \times a_3 R$, or a cylinder with elliptical base with semi-axis $a_1 R$ and $a_2 R$, respectively. E.g. $r(z, a; x) \equiv r_b(z; x) := [\sum_{i=1}^3 (x_i - z_i)^2]^{\frac{1}{2}}$ for a ball and $r(z, a; x) \equiv r_c(z, a; x) := [\sum_{i=1}^2 (\frac{x_i - z_i}{a_i})^2]^{\frac{1}{2}}$ for a cylinder. In line with the asymptotics of the phase field approach, see Sect. 1, the interfacial thickness for v is not less than $\gamma\pi$. For the initial data u^0 to (P) we chose either (i) one void or (ii) two voids; that is,

$$\text{(i) } u^0(x) = v(z, a, R; x) \quad \text{or} \quad \text{(ii) } u^0(x) = v(z, a, R; x) + v(\tilde{z}, \tilde{a}, \widetilde{R}; x) - 1. \tag{5.2}$$

For the iterative algorithms we set $U_\varepsilon^0 = \pi^h u^0$ and as initial profile for the chemical potential we set $W_\varepsilon^0 = -\gamma \Delta^h U_\varepsilon^0 - \gamma^{-1} U_\varepsilon^0$, i.e. $\underline{W}_\varepsilon^0 = M^{-1}(\gamma B \underline{U}_\varepsilon^0 - \gamma^{-1} M \underline{U}_\varepsilon^0)$. We chose the tolerance $tol = 10^{-8}$ as the stopping criterion for both the block Gauss–Seidel and Uzawa algorithms. For the computation of the second Uzawa substep (4.7b) we used a W-cycle multigrid with 1 pre-, in- and post-smoothing step. The multigrid iterations for the solution of (4.7b) were terminated when the tolerance tol was reached in the l^2 norm of the residual on the finest grid.

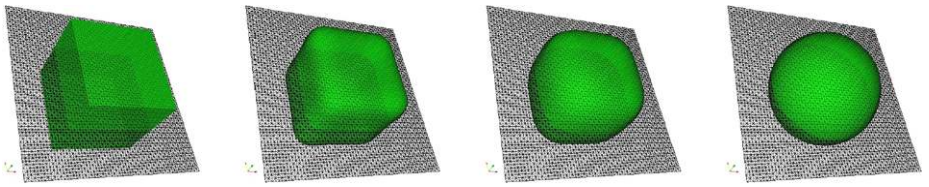

Fig. 2 ($\alpha = 0$) Zero level sets for $U_\varepsilon(x,t)$, with a cut through the mesh at $x_3 = 0$, at times $t = 0, 10^{-5}, 5 \times 10^{-5}, T = 0.001$

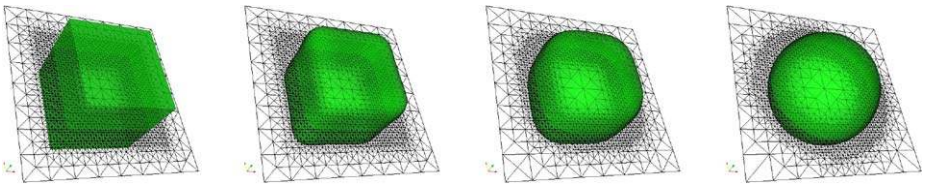

Fig. 3 ($\alpha = 0$) Zero level sets for $U_\varepsilon(x,t)$, with a cut through the mesh at $x_3 = 0$, at times $t = 0, 10^{-5}, 5 \times 10^{-5}, T = 0.001$

Our first computation is for the scheme ($\mathrm{P}_\varepsilon^{h,\tau}$) and shows the evolution of a cube, with side length $R = 0.5$, to a ball under motion by surface diffusion, see Fig. 2. The regularization parameter was chosen as $\varepsilon = 10^{-5}$, with the remaining parameters given by $\alpha = 0$, $\gamma = \frac{1}{6\pi}$, $\tau = 5 \times 10^{-6}$, $T = 0.001$. For this computation we used a fixed uniform triangulation. It was obtained by partitioning the domain $\Omega = (0,1)^3$ into cubes with side lengths $h = \frac{1}{64}$, with each cube being further subdivided into six generic right-angled tetrahedra, recall assumption (A). In general, the assumption (A) can only be guaranteed for such uniformly refined meshes. On the other hand, in practice one would like to employ highly adaptive triangulations that use a fine mesh along the interface and a coarse mesh away from it. Unfortunately such triangulations will in general always contain tetrahedra which do not satisfy assumption (A). Hence the scheme ($\mathrm{P}_\varepsilon^{h,\tau}$) can no longer be used in these situations. That is why we compared the results in Fig. 2 to results from the same computation on an adaptive grid for the scheme ($\widetilde{\mathrm{P}}^{h,\tau}$). The adaptive mesh was obtained from the mesh refinement strategy described below with parameters $N_f = 64$ and $N_c = 2$. The results in Fig. 3 are graphically indistinguishable from the results obtained with the scheme ($\mathrm{P}_\varepsilon^{h,\tau}$). However, since the triangulation is now adaptive and since the scheme ($\widetilde{\mathrm{P}}^{h,\tau}$) only needs to solve for the solution $\{U^n, W^n\}$ inside the interfacial region, the latter computation was approximately 2.7 times faster, where we used the iterative scheme (4.7a,b) in both cases. That is why for all our subsequent numerical simulations, we used the approximation ($\widetilde{\mathrm{P}}^{h,\tau}$).

For the implementation of our schemes, we used the adaptive finite element code Alberta, see [30], and we adapted the adaptive mesh approach from BNS to three space dimensions. We implemented a mesh refinement that generated a fine mesh along the interface and a relatively coarse mesh away from the interface. For the mesh refinement strategy we assume, for simplicity, that $L_1 \geq L_2 \geq L_3$ and that L_1 and L_2 are a multiples of L_3. We choose two parameters $N_f > N_c$ and set $h_f = \frac{2L_3}{N_f}$, $h_c = \frac{2L_3}{N_c}$. Then we set $vol_f = \frac{h_f^3}{6}$ and $vol_c = \frac{h_c^3}{6}$, i.e. the volumes of a tetrahedron with three right-angled and isosceles faces with side lengths h_f and h_c, respectively. We start with an initial partition $\mathcal{T}^0$ consisting of uniform tetrahedra for which $vol(\sigma) \leq vol_f$ and fix the parameters $\delta_f = tol$ and $\delta_c = tol \times 10^{-2}$, where tol is the prescribed tolerance. Then for $n \geq 1$ given U_ε^{n-1} and a partition $\mathcal{T}^{n-1}$, a tetrahedron is

Table 1 Computation times for different values of h, with $\gamma = \frac{1}{12\pi}$ fixed

N_f	τ	GS	Uzawa	Ratio
32	1E−05	9 m 40 s	11 m 20 s	0.85
64	4E−06	252 m	146 m	1.72
128	1E−06	14227 m	3460 m	4.11

Table 2 Computational times for different values of γ

γ	N_f	τ	GS	Uzawa	Ratio
$\frac{1}{3\pi}$	32	1E−05	93 m	30 m	3.1
$\frac{1}{6\pi}$	64	4E−06	853 m	259 m	3.29
$\frac{1}{12\pi}$	128	1E−06	14227 m	3460 m	4.11

marked for refinement if it satisfies

$$\eta_\sigma := \left|\min_{x\in\overline{\sigma}} |U_\varepsilon^{n-1}(x)| - 1\right| > \delta_f.$$

If a marked tetrahedron's volume satisfies $vol(\sigma) \geq 2vol_f$, it is refined via bisectioning of its longest edge. An element is marked for coarsening if it satisfies $vol(\sigma) \leq \frac{1}{2}vol_c$ and $\eta_\sigma < \delta_c$. After the initial mesh is obtained, the number of refined or coarsened elements on the next time levels is quite small. The above procedure ensures that the active nodes are always in the fine mesh region. Moreover, we observed in practice that on choosing $h_f \leq \frac{\gamma\pi}{10}$ the adapted mesh is guaranteed to have at least 6 mesh points across the interface.

Throughout, we used uniform time stepping with step size τ of the order $\mathcal{O}(h^2)$ and set $N_c := \frac{1}{8}N_f$, unless stated otherwise.

5.1 Comparison of Gauss–Seidel and Uzawa-Multigrid Schemes

In this section we compare the two iterative solvers (4.2a,b) and (4.7a,b). In line with the results obtained in [21], the number of iterations of the Uzawa-Multigrid algorithm was independent from the mesh size. We used the PGS method for the computation of the first Uzawa substep since it was faster than the MMG method in all our experiments. On average it reached convergence of the coincidence set after about 3 iterations. Typically, the outer Uzawa iterations converged after about 3 steps, even for the first time step $n = 1$. Note that this is a better behaviour than reported for the scheme in [21]. The multigrid solver for the second step (4.10) required 2 to 3 iterations on average per outer Uzawa iteration to converge. To illustrate the respective performances of the Gauss–Seidel and Uzawa schemes, we performed an experiment with $\alpha = 0$, $L_1 = 1.5$, $L_2 = L_3 = 0.5$. The experiment is for an initial $8 \times 1 \times 1$ prism with minor side length $R = 0.3$, see the first plot in Fig. 5 for the zero level set of U_ε^0 in the case $N_f = 128$ and $\gamma = \frac{1}{12\pi}$. We compared the computational times for different values of N_f with fixed final time $T = 2 \times 10^{-3}$ and either $\gamma = \frac{1}{12\pi}$ fixed, see Table 1, or varying values of γ, see Table 2. One can clearly see that the computations that used the Uzawa-Multigrid algorithm were several times faster than those with the Gauss–Seidel scheme and that the speedup factor increased with finer meshes.

For all the remaining computations in this paper, we employ the Uzawa-multigrid scheme.

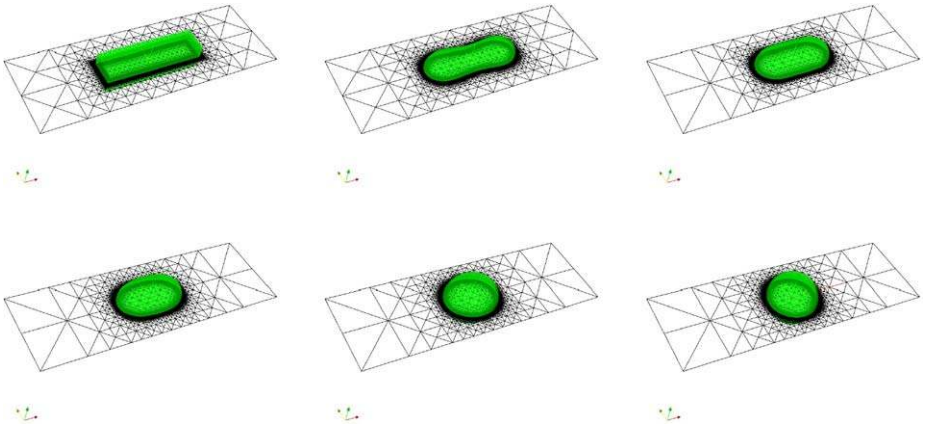

Fig. 4 ($\alpha = 0$) Zero level sets for $U_\varepsilon(x,t)$, with a cut through the mesh at $x_3 = 0$, at times $t = 0, 0.001, 0.005, 0.01, 0.015, T = 0.06$

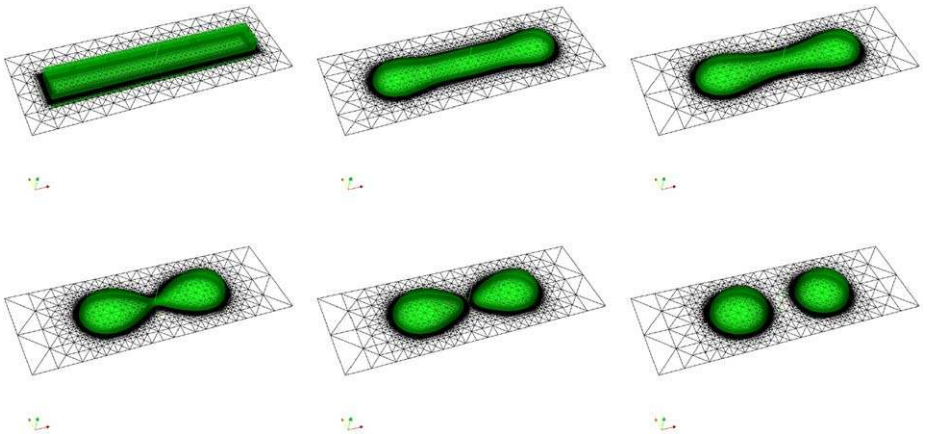

Fig. 5 ($\alpha = 0$) Zero level sets for $U_\varepsilon(x,t)$, with a cut through the mesh at $x_3 = 0$ at times $t = 0, 0.0015, 0.003, 0.00505, 0.0051, T = 0.006$

5.2 Surface Diffusion

In this section, we report on numerical experiments for the approximation (2.32a–c) with $\alpha = 0$. That is, in the limit $\gamma \to 0$, these computations model motion by surface diffusion, (1.6) with $\alpha = 0$. It is well known, that motion by surface diffusion for a compact two dimensional hypersurface in $\mathbb{R}^3$ can lead to pinch off, a topological change that cannot occur for a simple curve in two space dimension.

We demonstrate this phenomena with the following two experiments, with the domain parameters $L_1 = 1.5$, $L_2 = L_3 = 0.5$. The first experiment, see Fig. 4, describes the evolution of a $4 \times 1 \times 1$ prism, with minor side length $R = 0.3$, to a ball. That is, the zero level set of U_ε undergoes no change of topology. The parameters for the computation were $\gamma = \frac{1}{12\pi}$, $T = 0.06$, $N_f = 128$, $N_c = 2$, $\tau = 10^{-6}$.

However, if the initial prism is chosen sufficiently long, then pinch off occurs. We demonstrate this with the next experiment. The initial condition is a $8 \times 1 \times 1$ prism with minor

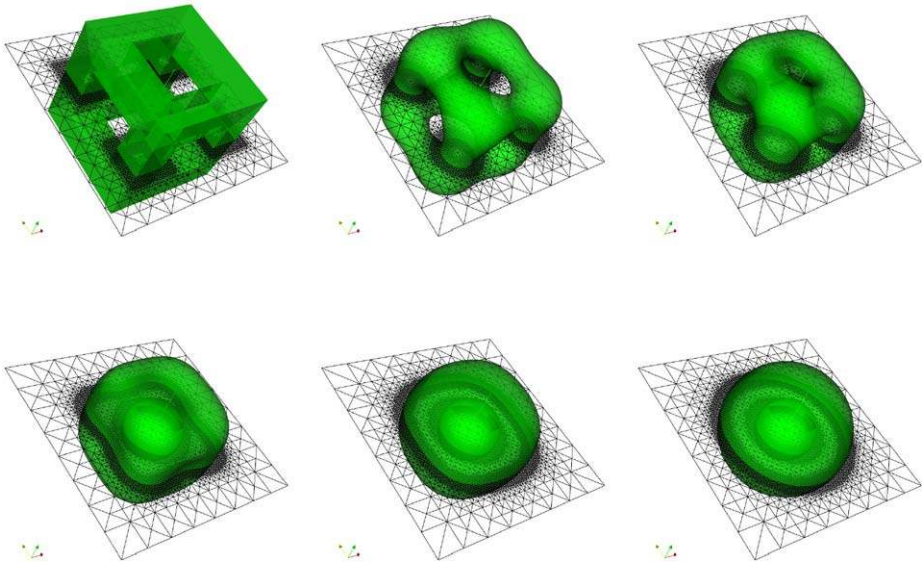

Fig. 6 ($\alpha = 0$) Zero level sets for $U_\varepsilon(x,t)$, with a cut through the mesh at $x_3 = 0$ at times $t = 0, 1.5 \times 10^{-4}, 3.5 \times 10^{-4}, 4 \times 10^{-4}, 4.5 \times 10^{-4}, 10^{-3}$

side length $R = 0.3$, and the other parameters were taken as in the previous example. The computation leads to a pinch off in finite time, see Fig. 5. A computation for a direct approximation of the same evolution can be found in [3, Fig. 10], and our results appear to be in good agreement (after a proper rescaling in time). However, we note that the direct method in [3] cannot compute beyond the change of topology, something that our phase field approach can.

In the next example, we show a more complicated surface diffusion flow. The evolution of a cage-like initial profile, that is made up of twelve $4 \times 1 \times 1$ prisms with minor side lengths $R = 0.15$, to a hollow ball undergoes a change in topology, when the six faces of the cage merge together. From a geometrical point of view, the surface undergoes an evolution from a genus 5 to two genus 0 surfaces. See Fig. 6 for the results, where we used the parameters $\gamma = \frac{1}{12\pi}$, $T = 10^{-3}$, $\tau = 10^{-6}$, $N_f = 128$, $N_c = 2$, $L_1 = L_2 = L_3 = 0.5$. Observe that a computation for a direct approximation of the same evolution is given in [11, Fig. 15], but once again the direct method employed there cannot compute beyond the change of topology.

5.3 Void Electromigration

The first electromigration experiment was computed with the following parameters: $\alpha = 114\pi$, $\gamma = \frac{1}{12\pi}$, $L_1 = 1$, $L_2 = L_3 = 0.5$, $T = 5 \times 10^{-4}$, $\tau = 10^{-7}$. The initial profile models a cylindrical void aligned with the x_3-axis and penetrating the conductor material. That is, we chose the initial profile (5.2)(i), with $r = r_c$ in (5.1) and $a = (1,1,1)^T$, $R = 0.375$, $z = (-0.5, 0, 0)^T$. The mesh refinement parameters were $N_f = 128$, $N_c = 16$. We note the excellent agreement between our results in Fig. 7, and the corresponding two dimensional results in [9, Fig. 2]. Moreover, the results confirm that an initial void that is invariant in the x_3-direction remains invariant throughout, if the electric field does not vary with x_3, see also [34].

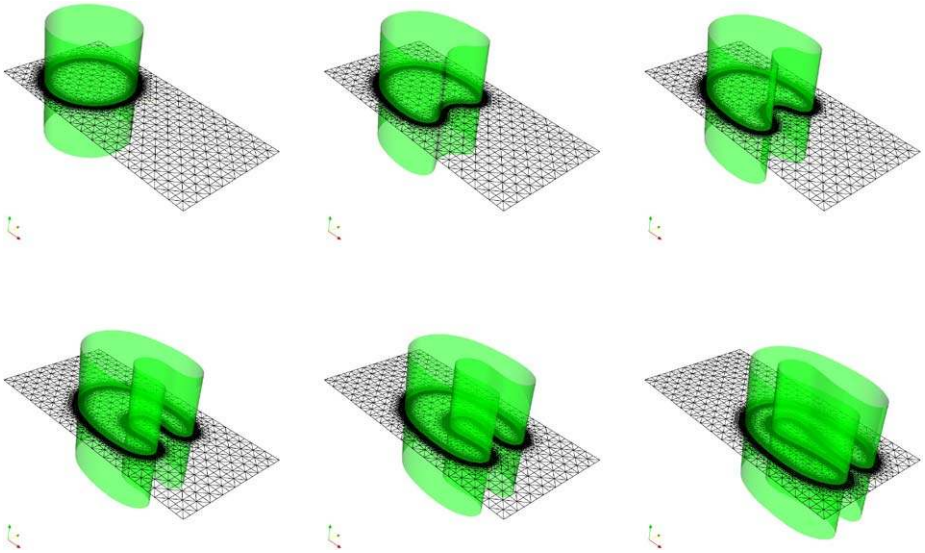

Fig. 7 ($\alpha = 114\pi$) Zero level sets for $U_\varepsilon(x,t)$, with a cut through the mesh at $x_3 = 0$, at times $t = 0, 8\times10^{-5}, 1.2\times10^{-4}, 2\times10^{-4}, 2.4\times10^{-4}, 3.6\times10^{-4}$

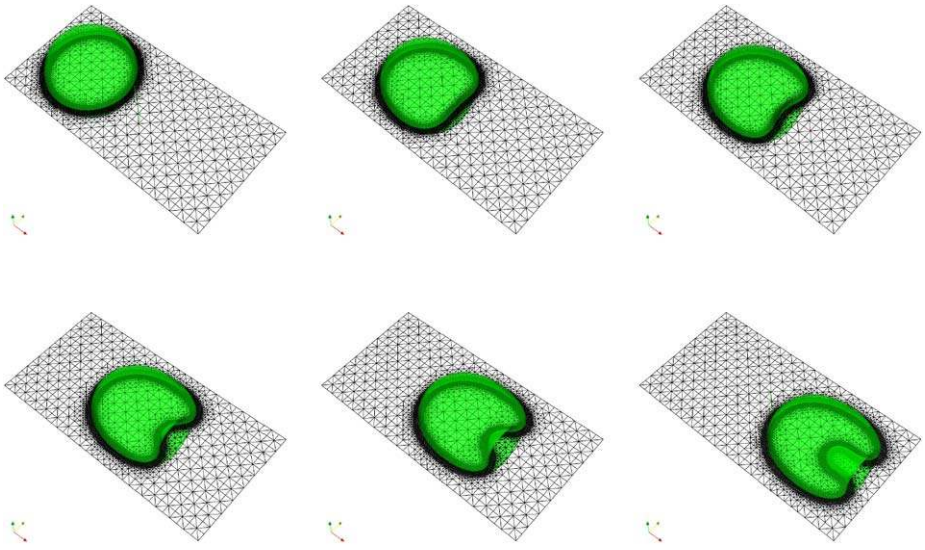

Fig. 8 ($\alpha = 114\pi$) Zero level sets for $U_\varepsilon(x,t)$, with a cut through the mesh at $x_3 = 0$, at times $t = 0, 8\times10^{-5}, 1.2\times10^{-4}, 2\times10^{-4}, 2.4\times10^{-4}, 3.6\times10^{-4}$

The next experiment illustrates a fully three dimensional situation. In particular, we choose the initial void in the shape of a ball, with the initial void boundary given by a closed compact hypersurface. We understand that the direct method in [34] cannot model this situation. For our computation we take the same parameters as in the previous simulation and start with a ball-shaped void of radius $R = 0.375$ centred at $z = (-0.5, 0, 0)^T$. It can be seen from the results depicted in Fig. 8, that for the same strength of the electric field,

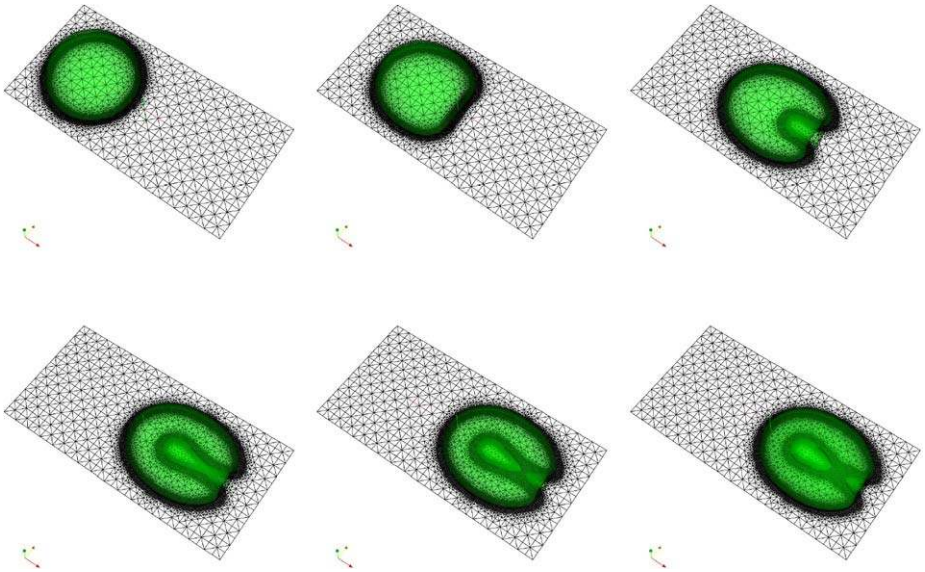

Fig. 9 ($\alpha = 300\pi$) Zero level sets for $U_\varepsilon(x,t)$, with a cut through the mesh at $x_3 = 0$, at times $t = 0, 2.5 \times 10^{-5}, 7.5 \times 10^{-5}, 1.15 \times 10^{-4}, 1.2 \times 10^{-4}, 1.25 \times 10^{-4}$

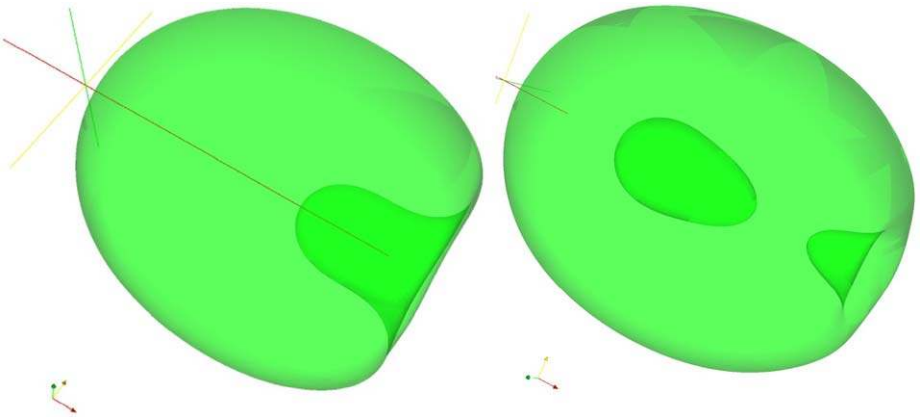

Fig. 10 Details of the zero level set of $U_\varepsilon(x,t)$ for $\alpha = 114\pi$, at time $t = 3.6 \times 10^{-4}$, and for $\alpha = 300\pi$, at time $t = 1.25 \times 10^{-4}$

the void undergoes relatively smaller deformations, compared to the penetrating cylindrical void in Fig. 7. However, when the strength of the electric field is increased to $\alpha = 300\pi$, the changes in the shape of the void are more dramatic. As can be seen from the results depicted in Fig. 9, now the void moves faster through the conductor, and it exhibits larger variations in its geometry. Eventually, this leads to a change in topology, with the void enclosing some material. For a close comparison, we present the zero level sets of the solution for $\alpha = 114\pi$ and $\alpha = 300\pi$ at times $t = 3.6 \times 10^{-4}$, and $t = 1.25 \times 10^{-4}$, respectively, in Fig. 10.

The last two experiments illustrate the interaction of two voids for two different strengths of the electric field. The first experiment corresponds to the two dimensional simulations in

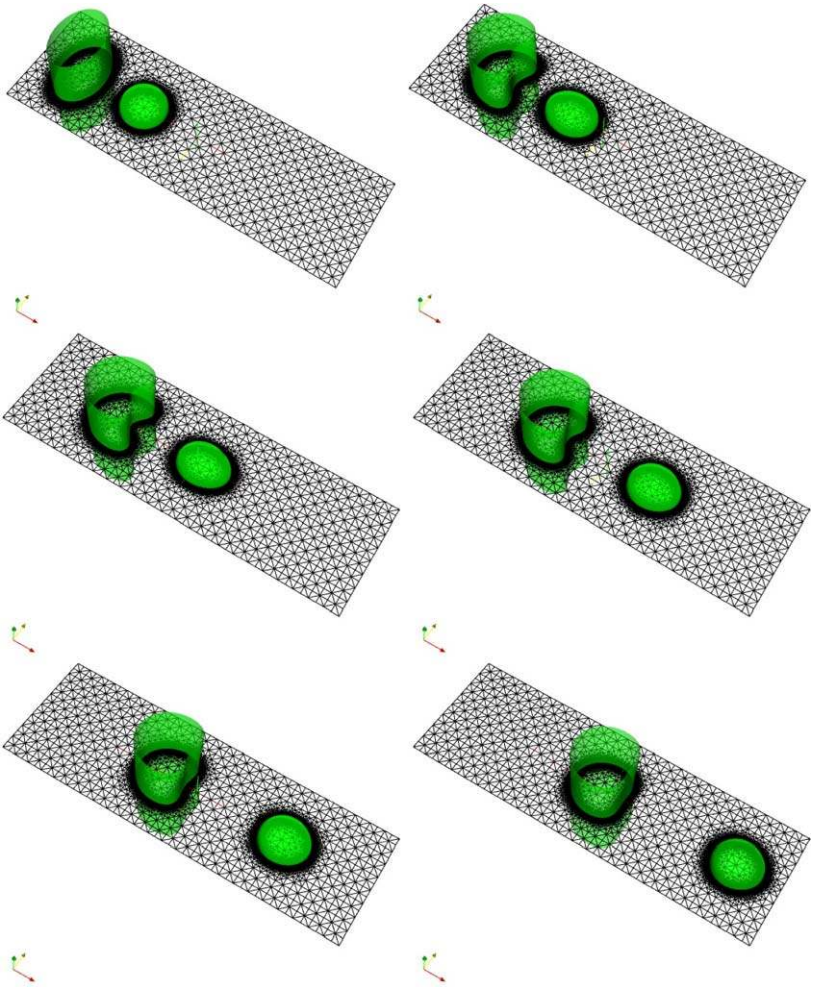

Fig. 11 ($\alpha = 64\pi$) Zero level sets for $U_\varepsilon(x,t)$, with a cut through the mesh at $x_3 = 0$, at times $t = 0, 10^{-4}, 2.6 \times 10^{-5}, 4.2 \times 10^{-5}, 5.8 \times 10^{-4}, 7.4 \times 10^{-4}$

[9, Fig. 8] and [24, Fig. 10]. In particular, the $x_3 = 0$ cut of our initial condition corresponds exactly to the two dimensional computations there, but here we choose the smaller void to be not penetrating in the x_3 direction. As initial condition we choose (5.2)(ii) with $r = r_c$ and $a = (1, 1.5, 1)^T$, $R = 0.2$, $z = (-1.1, 0, 0)^T$, and $\tilde{r} = r_b$ and $\tilde{R} = 0.2$, $\tilde{z} = (-0.5, 0, 0)^T$, respectively, in (5.1); i.e. a penetrating cylindrical void with elliptic base with a smaller ball-shaped void in front. The other parameters for the computation were $\alpha = 64\pi$, $\gamma = \frac{1}{12\pi}$, $L_1 = 1.5$, $L_2 = L_3 = 0.5$, $T = 7.4 \times 10^{-4}$, $\tau = 10^{-7}$, $N_f = 128$, $N_c = 16$. The results in Fig. 11 show that the penetrating void exhibits only very little variation of its geometry in the x_3 direction, while both voids move separately through the conductor. Moreover, the results differ dramatically from the two dimensional computations in [9, Fig. 8] and [24, Fig. 10]. This suggests, that for this particular situation a simplified two dimensional model is not sufficient.

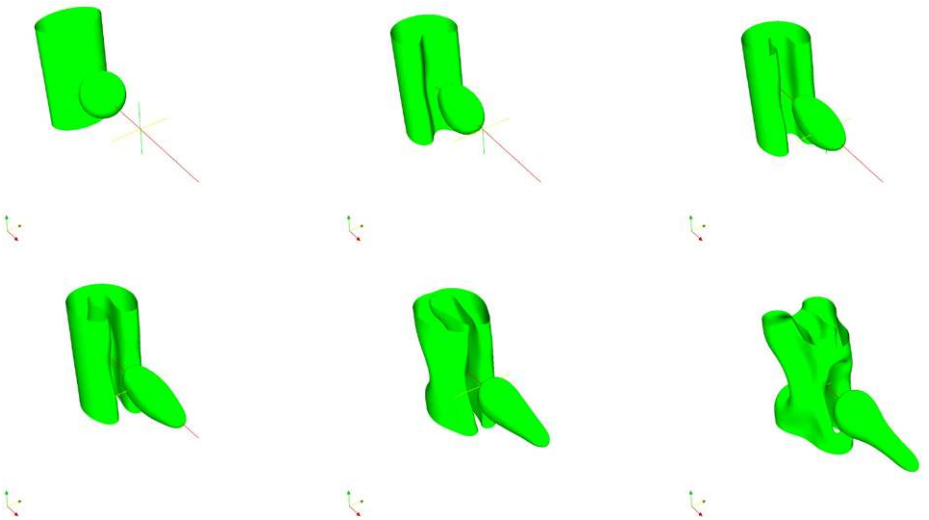

Fig. 12 ($\alpha = 120\pi$) Zero level sets for $U_\varepsilon(x,t)$ at times $t = 0, 7 \times 10^{-5}$, 1.3×10^{-4}, 1.9×10^{-4}, 2.3×10^{-4}, 2.7×10^{-4}

This is further underlined by the final experiment, where we kept all the parameters fixed, except $\alpha = 120\pi$, $\tilde{z} = (-0.6, 0, 0)^T$ and $T = 2.7 \times 10^{-4}$. The evolution for this stronger electric field leads to topological changes and produces rather complex three dimensional geometries that vary dramatically in the x_3 direction, see Fig. 12. Clearly, in situations like that a simplified two dimensional model is not able to capture the true character of the evolution.

References

1. Baňas L, Nürnberg R: A multigrid method for the Cahn–Hilliard equation with obstacle potential (2008, submitted)
2. Baňas L, Nürnberg R: Phase field computations for surface diffusion and void electromigration in $\mathbb{R}^3$. Comput. Vis. Sci. (2008). doi:10.1007/s00791-008-0114-0
3. Bänsch, E., Morin, P., Nochetto, R.H.: A finite element method for surface diffusion: the parametric case. J. Comput. Phys. **203**, 321–343 (2005)
4. Barrett, J.W., Blowey, J.F.: Finite element approximation of a degenerate Allen–Cahn/Cahn–Hilliard system. SIAM J. Numer. Anal. **39**, 1598–1624 (2001)
5. Barrett, J.W., Blowey, J.F., Garcke, H.: Finite element approximation of a fourth order nonlinear degenerate parabolic equation. Numer. Math. **80**, 525–556 (1998)
6. Barrett, J.W., Blowey, J.F., Garcke, H.: Finite element approximation of the Cahn–Hilliard equation with degenerate mobility. SIAM J. Numer. Anal. **37**, 286–318 (1999)
7. Barrett, J.W., Blowey, J.F., Garcke, H.: On fully practical finite element approximations of degenerate Cahn–Hilliard systems. M2AN Math. Model. Numer. Anal. **35**, 713–748 (2001)
8. Barrett, J.W., Langdon, S., Nürnberg, R.: Finite element approximation of a sixth order nonlinear degenerate parabolic equation. Numer. Math. **96**, 401–434 (2004)
9. Barrett, J.W., Nürnberg, R., Styles, V.: Finite element approximation of a phase field model for void electromigration. SIAM J. Numer. Anal. **42**, 738–772 (2004)
10. Barrett, J.W., Nürnberg, R., Warner, M.R.E.: Finite element approximation of soluble surfactant spreading on a thin film. SIAM J. Numer. Anal. **44**, 1218–1247 (2006)
11. Barrett, J.W., Garcke, H., Nürnberg, R.: On the parametric finite element approximation of evolving hypersurfaces in $\mathbb{R}^3$. J. Comput. Phys. **227**, 4281–4307 (2008)

12. Blowey, J.F., Elliott, C.M.: The Cahn–Hilliard gradient theory for phase separation with non-smooth free energy. Part II: Numerical analysis. Eur. J. Appl. Math. **3**, 147–179 (1992)
13. Brandts, J., Křížek, M.: Gradient superconvergence on uniform simplicial partitions of polytopes. IMA J. Numer. Anal. **23**, 489–505 (2003)
14. Cahn, J.W., Elliott, C.M., Novick-Cohen, A.: The Cahn–Hilliard equation with a concentration dependent mobility: motion by minus the Laplacian of the mean curvature. Eur. J. Appl. Math. **7**, 287–301 (1996)
15. Chopp, D.L., Sethian, J.A.: Motion by intrinsic Laplacian of curvature. Interfaces Free Bound. **1**, 107–123 (1999)
16. Deckelnick, K., Dziuk, G., Elliott, C.M.: Computation of geometric partial differential equations and mean curvature flow. Acta Numer. **14**, 139–232 (2005)
17. Elliott, C.M., Garcke, H.: On the Cahn–Hilliard equation with degenerate mobility. SIAM J. Math. Anal. **27**, 404–423 (1996)
18. Feng, X., Prohl, A.: Numerical analysis of the Cahn–Hilliard equation and approximation of the Hele–Shaw problem. Interfaces Free Bound. **7**, 1–28 (2005)
19. Glowinski, R.: Numerical Methods for Nonlinear Variational Problems. Springer, New York (1984)
20. Glowinski, R., Lions, J.-L., Trémolières, R.: Numerical Analysis of Variational Inequalities. Studies in Mathematics and its Applications, vol. 8. North-Holland, Amsterdam (1981). Translated from the French
21. Gräser, C., Kornhuber, R.: On preconditioned Uzawa-type iterations for a saddle point problem with inequality constraints. In: Domain Decomposition Methods in Science and Engineering XVI. Lect. Notes Comput. Sci. Eng., vol. 55, pp. 91–102. Springer, Berlin (2007)
22. Grün, G.: On the convergence of entropy consistent schemes for lubrication type equations in multiple space dimensions. Math. Comput. **72**, 1251–1279 (2003)
23. Kornhuber, R.: Monotone multigrid methods for elliptic variational inequalities I. Numer. Math. **69**, 167–184 (1994)
24. Li, Z., Zhao, H., Gao, H.: A numerical study of electro-migration voiding by evolving level set functions on a fixed cartesian grid. J. Comput. Phys. **152**, 281–304 (1999)
25. Manservisi, S.: Numerical analysis of Vanka-type solvers for steady stokes and Navier–Stokes flows. SIAM J. Numer. Anal. **44**, 2025–2056 (2006)
26. Mayer, U.F.: A numerical scheme for moving boundary problems that are gradient flows for the area functional. Eur. J. Appl. Math. **11**, 61–80 (2000)
27. Mayer, U.F.: Numerical solutions for the surface diffusion flow in three space dimensions. Comput. Appl. Math. **20**, 361–379 (2001)
28. Mullins, W.W.: Theory of thermal grooving. J. Appl. Phys. **28**, 333–339 (1957)
29. Nürnberg, R.: Finite element approximation of some degenerate nonlinear parabolic systems. PhD thesis, University of London, London (2003)
30. Schmidt, A., Siebert, K.G.: ALBERT—software for scientific computations and applications. Acta Math. Univ. Comen. (N.S.) **70**, 105–122 (2000)
31. Schoberl, J., Zulehner, W.: On Schwarz-type smoothers for saddle point problems. Numer. Math. **95**, 377–399 (2003)
32. Simon, J.: Compact sets in the space $L^p(0, T; B)$. Ann. Math. Pura. Appl. **146**, 65–96 (1987)
33. Smereka, P.: Semi-implicit level set methods for curvature and surface diffusion motion. J. Sci. Comput. **19**, 439–456 (2003)
34. Zhang, Y.W., Bower, A.F., Xia, L., Shih, C.F.: Three dimensional finite element analysis of the evolution of voids and thin films by strain and electromigration induced surface diffusion. J. Mech. Phys. Solids **47**, 173–199 (1999)